Quantifying the $\delta^{15}N$ trophic offset in a cold-water scleractinian coral (CWC): implications for the CWC diet and coral $\delta^{15}N$ as a marine N cycle proxy

Josie L. Mottram[1], Anne M. Gothmann[2], Maria G. Prokopenko[3], Austin Cordova[3], Veronica Rollinson[1], Katie Dobkowski[4], Julie Granger[1]

[1]Department of Marine Sciences, University of Connecticut, Storrs, CT, 06340, USA
[2]Departments of Physics and Environmental Studies, St. Olaf College, Northfield, MN, 55057, USA
[3]Department of Geology, Pomona College, Claremont, CA, 91711, USA
[4]Department of Environmental Studies, Woodbury University, Burbank, CA, 91504, USA

Correspondence to: Anne M. Gothmann (gothma1@stolaf.edu)

Abstract. The nitrogen (N) isotope composition ($\delta^{15}N$) of cold-water corals is a promising proxy for reconstructing past ocean N cycling, as a strong correlation was found between the $\delta^{15}N$ of the organic nitrogen preserved in coral skeletons and the $\delta^{15}N$ of particulate organic matter exported from the surface ocean. However, a large offset of 8-9 ‰ between the $\delta^{15}N$ recorded by the coral and that of exported particulate organic matter remains unexplained. The 8-9 ‰ offset may signal a higher trophic level of coral dietary sources, an unusually large trophic isotope effect or a biosynthetic $\delta^{15}N$ offset between the coral's soft tissue and skeletal organic matter, or some combinations of these factors. To understand the origin of the offset and further validate the proxy, we investigated the trophic ecology of the asymbiotic scleractinian cold water coral *Balanophyllia elegans,* both in a laboratory setting and in its natural habitat. A long-term incubation experiment of *B. elegans* fed on an isotopically controlled diet yielded a canonical trophic isotope effect of 3.0 ± 0.1‰ between coral soft tissue and the *Artemia* prey. The trophic isotope effect was not detectably influenced by sustained food limitation. A long N turnover of coral soft tissue, expressed as an e-folding time, of 291 ± 15 days in the well-fed incubations indicates that coral skeleton $\delta^{15}N$ is not likely to track subannual (e.g. seasonal) variability of diet $\delta^{15}N$. Specimens of *B. elegans* from the subtidal zone near San Juan Channel (WA, USA) revealed a modest difference between soft tissue and skeletal $\delta^{15}N$ of 1.2 ± 0.6 ‰. The $\delta^{15}N$ of the coral soft tissue was 12.0 ± 0.6 ‰, which was ~6 ‰ higher than that of suspended organic material that was comprised dominantly of phytoplankton – suggesting that phytoplankton is not the primary component of *B. elegans'* diet. An analysis of size-fractionated net tow material suggests that *B. elegans* fed predominantly on a size class of zooplankton ≥ 500 μm, implicating a two-level trophic transfer between phytoplankton material and coral tissue. These results point to a feeding strategy that may result in an influence of regional food web structure on the cold-water coral $\delta^{15}N$. This factor should be taken into consideration when applying the proxy to paleoceanographic studies of ocean N cycling.

1 Introduction

35   Interactions between ocean circulation and nutrient cycling modulate the marine biological carbon pump,
36   the consequent partitioning of CO_2 between atmosphere and ocean, and thus influence planetary climate on
37   centennial to millennial time scales (Sigman and Boyle 2000). The marine nitrogen (N) cycle is highly sensitive
38   to these interactions, such that knowledge of modern and ancient ocean N cycling can help illuminate drivers of
39   past climate and contextualize modern global change (*e.g.*, Altabet et al., 1994; Francois et al., 1997; Robinson
40   and Sigman 2008; Sigman et al., 1999; Kast et al. 2019).

41   The main tool to investigate the oceanic N cycle history is the nitrogen (N) isotope composition (*i.e.*, the
42   $^{15}N/^{14}N$ ratio) of particulate organic nitrogen (PON) exported from the euphotic zone and preserved in various
43   paleo-archives, including bulk sedimentary N in anoxic sediments (*reviewed by* Robinson et al. 2023). Hereafter,
44   we express the $^{15}N/^{14}N$ ratio using delta notation ($\delta^{15}N$). The $\delta^{15}N$-PON recorded in paleo-oceanographic archives
45   reflects both regional N cycling processes and the balance of global ocean N source and sink terms (Sigman and
46   Fripiat 2019; Brandes and Devol 2002). In regions of the ocean where nitrate is quantitatively consumed, the
47   annually integrated $\delta^{15}N$-PON exported from the surface reflects the isotopic composition of thermocline nitrate
48   (Altabet et al. 1991). The latter is influenced by the circulation history of nitrate (*e.g.*, Marconi et al., 2015), by
49   regional N_2 fixation (*e.g.*, Casciotti et al. 2008; Knapp et al. 2008) and by water column denitrification (*e.g.,*
50   Pride et al., 1999; De Pol-Holz et al., 2007). In regions with incomplete consumption of surface nitrate, such as
51   Southern Ocean, the isotopic discrimination imparted during nitrate assimilation is reflected in the $\delta^{15}N$-PON,
52   which can be used to reconstruct the degree of surface nitrate consumption in the past (*e.g.,* Sigman et al., 1999;
53   Francois et al. 1997).

54   Accurate interpretation of the N cycle's paleo-history relies on the presumption that the $\delta^{15}N$-PON preserved
55   in various palaeoceanographic archives is impervious to organic matter diagenesis. Bulk sedimentary $\delta^{15}N$
56   measurements are thus generally inadequate in this respect, subject to post-depositional processes (Robinson et
57   al. 2012) – barring fast-accumulating organic-rich anoxic sediments with negligible contribution from terrestrial
58   sources (*e.g.*, Altabet et al., 2002; Ganeshram and Pedersen, 1998). To circumvent this limitation, several
59   "biological" archives of the $\delta^{15}N$-PON have been developed that are deemed resistant to diagenetic alteration.
60   These include the organic matter in in diatom frustules and foraminifera tests (*e.g.*, Ren et al., 2009; Robinson
61   and Sigman, 2008) and the organic matter in proteinaceous corals (*e.g.*, Sherwood et al. 2009; Williams and
62   Grottoli 2010). Recently, the $\delta^{15}N$ of organic N enclosed within the aragonite mineral lattice of asymbiotic
63   scleractinian (stony) cold-water corals (CWCs) has been found to reflect the $\delta^{15}N$-PON exported from the surface

64 ocean (Wang et al., 2014), offering an exciting new archive of marine N cycling (Wang et al. 2017; Li et al.,

65 2020, Studer et al., 2018; Chen et al. 2023). A robust cold-water coral archive of δ^{15}N-PON can complement the

66 existing suite of nitrogen proxies by reducing the potential biases inevitable for almost any individual proxy,

67 allowing for a broader geographic and temporal reconstruction, and increasing resolution of the proxy record.

68 Foremost, as with foraminifera and diatom shells, organic material trapped within the coral's original aragonite

69 mineral lattice is largely protected from diagenetic alteration (Drake et al. 2021), and compromised areas can be

70 avoided by inspecting the skeletons for contamination and recrystallization (*e.g.*, borings) using microscopic

71 techniques (Gothmann et al. 2015). CWCs have a broad geographic distribution, being present in all ocean basins

72 from the surface to 5000 m (Freiwald, 2002). CWCs also offer the potential to generate high-resolution records

73 extending relatively far back in time, and corals have continuous skeletal accretion that records ocean conditions

74 at the time of growth, so the analysis of multiple individuals provides enhanced temporal resolution of long-term

75 records (Robinson et al., 2014; Hines et al. 2015). Unlike sediments containing microfossils (e.g. diatoms and

76 foraminifera) CWC skeletons are not subject to bioturbation and absolute ages of this paleoarchive can be

77 determined with decadal precision on the time scales of glacial-interglacial climate variability through U-Th

78 series dating (Cheng et al., 2000; Goodfriend et al. 1992, Robinson et al., 2014, Li et al., 2020). Remarkably,

79 individual coral samples can archive multiple seawater properties, such that a single CWC specimen can

80 potentially be used to reconstruct deep (*e.g.*, Δ^{14}C, pH, temperature, and circulation proxies such as Ba/Ca

81 and εNd) and surface ocean conditions (δ^{15}N) at a precisely-known time (U-Th dating), making CWC unique as a

82 paleoceanographic archive (Robinson et al., 2014; Thiagarajan et al., 2014; Rae et al. 2018).

83   Yet an outstanding concern about the fidelity of the δ^{15}N of coral-bound organic N is a reported 8 - 9 ‰

84 offset between coral-bound δ^{15}N and the corresponding δ^{15}N-PON exported to regions of coral growth (Wang et

85 al. 2014). The magnitude of this offset substantially exceeds the 3 - 3.5 ‰ expected for a single trophic transfer

86 (Minagawa and Wada 1984), assuming CWC feed predominantly on algal material exported from the surface

87 ocean. Wang et al. (2014) explained the magnitude of the offset by arguing that CWCs feed on the more

88 abundant pool of surface-derived suspended organic material (SPOM), as the δ^{15}N SPOM at depth is typically

89 ~4-5‰ higher than that of sinking PON (Altabet 1988, Saino and Hattori, 1987). While CWCs are considered

90 generalists with regard to diet (e.g., Mortensen, 2001; Freiwald, 2002; Carlier et al., 2009; Maier et al. 2023), a

91 number of studies suggest that many species of CWC subsist predominantly on metazoan zooplankton prey (e.g.,

92 Naumann et al. 2011; Kiriakoulakis et al. 2005; Purser et al. 2010; Tsounis et al. 2010). A zooplankton diet

93 should result in an approximate two-level or more trophic transfer between surface PON and coral tissue (*e.g.*,

94 Sherwood et al. 2008), closer to the observed 8-9 ‰ offset, potentially rendering coral-bound δ^{15}N sensitive to

95 spatial and temporal differences in trophic-level food web structure. An alternative explanation for the offset is

96 that there is a large biosynthetic offset between the δ^{15}N of the CWC polyp and its skeletal tissue (Horn et al.

97 2011; Muscatine et al. 2005), assuming that CWCs' diet derives directly from sinking algal material from the

98 surface ocean. Otherwise, there could be an atypically large N isotope fractionation associated with the trophic-

99 level transfer between the coral diet and its tissue (>3-3.5‰), possibly borne out of intermittent starvation periods

100 (Doi et al., 2017), which is then passed on to the organic matrix within the coral skeleton. The gap in our

101 understanding of how corals record the δ^{15}N-PON exported form the surface ocean raises questions regarding the

102 consistency of the offset in space and time, and whether it is likely to differ among CWC species or due to intra-

103 specific variations in diet.

104   Due to the challenges of accessing deep-ocean environments, the trophic ecology of cold-water corals is

105 sparsely documented, yet is fundamental to understanding the role of CWCs in cold-water reef ecosystems and to

106 defining their utility as paleoceanographic archives of N cycling. The nature of the δ^{15}N offset between CWC

107 skeletal material and exported PON must be explained in order to further validate and potentially improve the use

108 of δ^{15}N of CWC skeletons as a proxy to reconstruct the history of exported PON and to further understand the

109 role of CWCs in benthic ecosystems. To this end, we studied *Balanophyllia elegans,* an asymbiotic scleractinian

110 cold-water coral found along the west coast of North America that grows as individual polyps (Fadlallah, 1983).

111 We investigated the following questions: a) Is there a large offset in δ^{15}N between coral polyp tissue and coral

112 skeletal tissue? b) Is there an unusually large trophic-level offset between coral tissue and coral diet? c) Does *B.*

113 *elegans* feed predominantly on suspended particulate organic matter (SPOM) *in situ*? or d) does *B. elegans* feed

114 predominantly on metazoan zooplankton, resulting in a two-level trophic transfer between coral tissue and N of

115 export? To evaluate question (a), we measured the δ^{15}N of tissue-skeleton pairs of coral samples collected in their

116 natural habitat. To evaluate question (b), we cultured *B. elegans* corals in the laboratory in experiments where

117 both the isotopic composition of food and the frequency of feeding was controlled. To evaluate questions (c) and

118 (d), we also investigated the δ^{15}N of various components of the food web at a field site where *B. elegans* are

119 found plentifully. Our observations offer novel insights on the growth and trophic ecology of *B. elegans*,

120 providing unique new data on the N metabolism of CWC and their feeding ecology. We contextualize our

121 conclusions to inform the use of CWC archives as a paleo-proxy for marine N cycling and ocean

122 biogeochemistry.

123

2. Methods

2.1 Collection of live coral specimens

Individual specimens of the cold-water coral *Balanophyllia elegans* were collected during four sampling campaigns in March and June 2019, and September and November 2020 from the San Juan Channel near the University of Washington's Friday Harbor Laboratory off the coast of Washington State in the Salish Sea (48.5º N, -123.0º W; Figure 1). *B. elegans* is a solitary, asymbiotic cold-water cup coral native to the Pacific Northwest that can be found both in shallow rocky environments and at depths as great as 500 m (Durham and Barnard 1952). The genus *Balanophyllia* is cosmopolitan and fossil samples as old as Eocene in age have been used for paleoenvironmental study (Muhs et al. 1994; Gothmann et al., 2015; Gagnon et al. 2021). *B. elegans's* presence at near surface depths makes it an easy target for culture experiments, and *Balanophyllia sp.* can be found co-occurring with the similar but more widely applied cold-water coral archive, *Desmophyllum dianthus* (Margolin et al. 2014). Therefore, we consider the asymbiotic *Balanophyllia sp.* to be generally representative of other deep cold-water coral species.
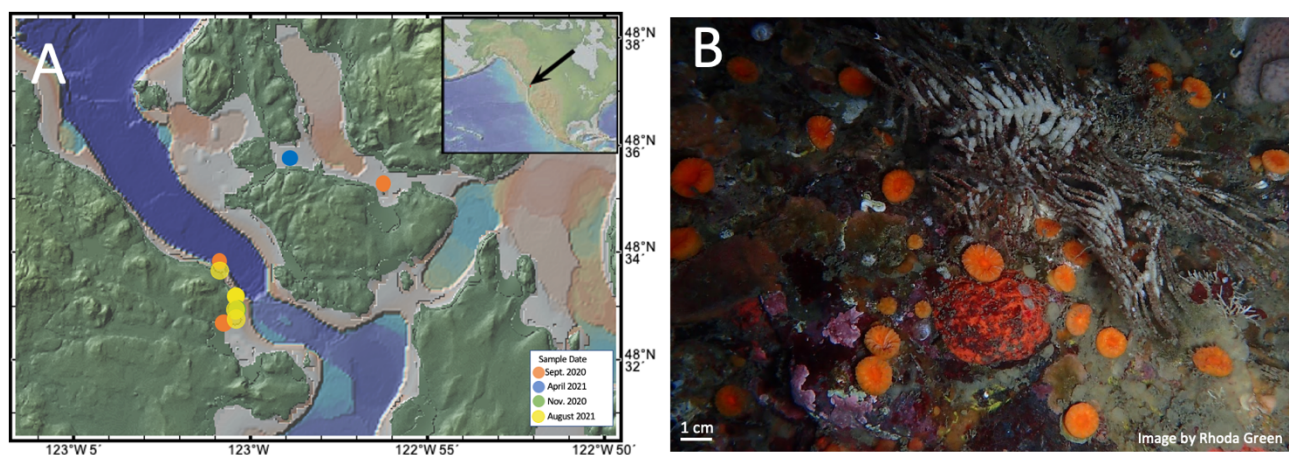
Figure 1. (a) Map of the San Juan Islands indicating the collection site of *B. elegans* specimens and hydrographic measurements (created using http://www.geomapapp.org, Ryan et al. 2009). Inset shows where the San Juan Islands are situated within North America. (b) Image of *B. elegans* from the San Juan Channel near Friday Harbor Labs taken by Rhoda Green.

B. elegans specimens were collected at 10 to 20 m depth by divers who gently removed the corals from vertical rock walls using blunt-tipped diving knives. Of the live corals collected, a subset was immediately frozen at -18ºC for N isotope ratio analyses of soft tissue and organic matter bound in the coral skeleton matrix. Live specimens were shipped overnight in small bags of seawater on ice to St. Olaf College (Minnesota, USA). Corals

were cleaned by gently scraping the exposed skeleton with dental tools to remove encrusting organisms and placed in incubation bottles with artificial seawater for recovery prior to feeding experiments (described below).

2.2 Live coral maintenance

Live *B. elegans* corals were maintained in artificial seawater medium prepared from nitrate-free Instant Ocean® Sea Salt. Salts were dissolved in deionized water to a salinity of 28.0 ± 0.25 – akin to the conditions at the collection site (Murray et al., 2015) – and sparged with air to achieve atmospheric equilibrium. The pH of the seawater was measured with a YSI brand 4130 pH probe and adjusted using dilute (0.1 N) hydrochloric acid or sodium hydroxide to 8.14 ± 0.05, slightly higher than *in-situ* conditions to promote skeletal growth. Batch seawater was then allotted to 2 L airtight polypropylene bottles to incubate single coral polyps. Bottles were pre-cleaned with fragrance-free soap and multiple rinses of deionized water. The salinity, pH, and temperature in the incubation bottles were monitored using YSI brand probes (4310(W) conductivity cell and pH probe, respectively) as well as dissolved oxygen concentrations using an optical sensor (FDO 4410; Figure S1); a Multilab 4010-3w was used as the digital meter for the sensors. The bottles containing individual corals were randomly distributed among three recirculating water baths maintained at a constant temperature of 12.5 ± 0.2 ºC, akin to the conditions at the collection site (Murray et al., 2015). Small but quasi-systematic differences of $\pm$ 0.3˚C were observed among the three recirculating tanks (Figure S2). Corals were sustained on a diet of *Artemia salina* nauplii (described below), fed twice a week to ensure maximum growth (Crook et al., 2013). Seawater in the incubation bottles was replaced twice a week after the corals were fed, based on observations indicating that seawater pH in the bottles decreased slightly but significantly by ~0.03 pH units over three days due to coral respiration (statistical analysis was performed with RStudio; Welch two sample t-test; $t(515.07)= 12.8$; p-value < 0.01; Figure S3). Dissolved oxygen concentrations remained near atmospheric equilibrium at concentration of 7.5 ± 0.3 mg L^{-1} (Figure S1). Nitrate concentrations in the bottles were also monitored from samples taken during each water change, in the freshly prepared seawater and in spent seawater, revealing low variability in NO_3^- concentration of 0.7 ± 0.3 µmol L^{-1} (Figure S4). Nitrate concentrations in the incubations were notably lower than ambient levels at the collection site, where concentration were ~25 µmol L^{-1}, ensuring that the coral's only source of nitrogen was the *Artemia* diet (Murray et al., 2015).

2.3 Coral culture experiments

2.3.1 Experiment to quantify the trophic isotope effect

The corals were acclimated to precise incubation conditions for approximately 20 hours before initiating feeding experiments. To assess the δ^{15}N of coral soft tissue compared to that of its food source, four experimental groups of individual *B. elegans* corals were fed respective diets of *Artemia salina* nauplii with different δ^{15}N values, twice per week for 530 days (Spero et al., 1993). Unhatched *Artemia salina* sourced from specific geographic locations have widely different δ^{15}N values, owing to the different N isotope dynamics of the environments from which they were collected, which makes these organisms useful for trophic studies (Spero et al. 1993). Eighteen coral specimens were fed *Artemia* nauplii hatched from cysts from the Great Salt Lake (Reference Code: GSL) with a δ^{15}N of 17.0 ± 0.3 ‰. Twelve corals were fed hatched nauplii from Lake Ulzhay in Russia (Reference Code: 1816) with a δ^{15}N of 13.8 ± 0.4 ‰. Twelve corals were fed hatched nauplii from Vinh Chau in Vietnam (Reference Code: 1805) with a δ^{15}N of 9.9 ± 0.3‰. Twelve corals were fed hatched nauplii from Tibet (Reference Code: 1808) with δ^{15}N of 6.3 ± 0.2‰. The GSL *Artemia* was procured from Aquatic Foods California Blackworm Co. (Great Salt Lake), whereas all other *Artemia* were obtained from the Artemia Reference Center (Ghent, Belgium). The δ^{15}N of the diet for each treatment was calculated as the mean value measured from each group of unhatched cysts and hatched nauplii (Table S2 and S3).

Fresh batches of nauplii were hatched from *Artemia* cysts at approximately monthly intervals, filtered into a concentrated suspension, stored frozen at -18ºC, and thawed immediately before feeding to the corals. Due to low hatch rates of the *Artemia* group 1808, corals in that treatment group were fed nauplii harvested from decapsulated *Artemia* cysts from day 151 (November 19, 2019) to 245 (February 22, 2020). The δ^{15}N of the hatched nauplii ranged from 6.3 ± 0.2 to 17.0 ± 0.3 ‰ (measured by EA-IRMS; Table S2). The δ^{15}N of the nauplii did not change significantly over prolonged storage of several months in the freezer (ANOVA test; F(1) = 0.07, p-value = 0.80; Figure S5). *Artemia* nauplii had a statistically indistinguishable molar C:N ratios among regional groups, averaging 6.0 ± 0.6 (ANOVA test; F(3) = 0.31; p-value = 0.82, Table S3). These results show that there was limited variability in the diet of corals due to freezer storage and hatching of multiple individual batches of *Artemia* (Table S2, S3, Figure S5).

Corals were fed their respective nauplii diets by transferring coral individuals from their incubation bottle to a small dish filled with artificial seawater with minimal exposure to air so as not to stress the corals. Each coral was fed 20 µL of thawed nauplii suspension by pipetting the food directly into their oral cavity, making it possible to visually ensure complete consumption and thus minimize variability in feeding rates. Each coral was

returned to its bottle with a fresh allotment of seawater when its mouth had remained closed for several minutes, signifying that it was finished eating (Figure 2).

After a shift in the $\delta^{15}N$ of diet, it is expected that coral tissue $\delta^{15}N$ will evolve as a function of time until the composition of tissue reaches an equilibrium in line with the new diet. In order to assess the rate (referred to here as the isotopic turnover time) at which this evolution occurs, individual corals were sacrificed at discrete intervals throughout the experiment. Corals were always sacrificed three days after feeding to ensure that no food remained in the oral cavity. The corals were removed from their bottles and rinsed with artificial seawater. The coral tissue was then separated from the skeleton using a fine stream of compressed air. The tissue and skeleton were frozen at -18°C and stored separately until processed for isotope ratio analyses.
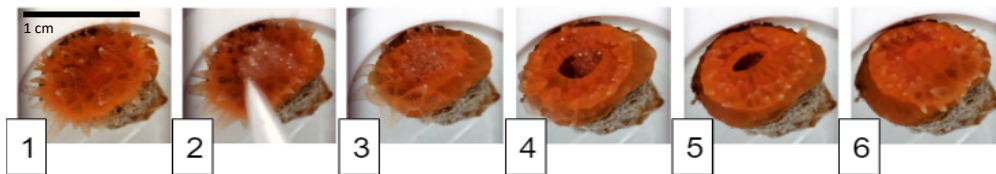
Figure 2. Photo illustration of a coral feeding sequence. Photo 1 shows coral before food is given. Photo 2 shows food being pipetted onto coral mouth. Photos 3 through 6 show the coral feeding as the mouth opens to engulf food and closes when finished, about 15 minutes in total. Corals are ~1 cm in diameter.

2.3.2   Experiment to evaluate the effects of starvation conditions

An additional 522-day feeding experiment was performed to assess the influence of starvation on the $\delta^{15}N$ of the coral soft tissue. Live corals collected during a sampling campaign at the end of November 2020 and shipped live to St. Olaf College were randomly assigned to two treatment groups (starved and not-starved). Corals in the starved treatment were fed at 25% of our normal feeding frequency, or every two weeks, whereas those in the not-starved treatment were fed twice a week. These feeding regimes were chosen based on the work of Crook et al. (2013) and Beauchamp et al. (1989), who assumed feeding every 3 days to represent plentiful food supply and feeding every 21 days (close to our starvation condition) to represent minimal maintenance food supply. Both groups were fed *Artemia* nauplii with a $\delta^{15}N$ of 9.9 ± 0.3 ‰, approximately 3 ‰ lower than the coral tissue of average *B. elegans* collected from Friday Harbor, and thus presumably closest in $\delta^{15}N$ to what the corals is eating in the wild given a canonical trophic isotope effect. Coral incubations and feedings were conducted as described above. Individuals were sacrificed over the course of the 522-day experiment, and tissue samples were frozen at -18°C until isotope analysis.

2.4 Coral preparation for isotope ratio analyses

Frozen coral tissue samples (and hatched nauplii) were freeze-dried using a Labconco FreeZone 4.5 and then powdered using a mortar and pestle. The samples were sent to the University of Connecticut, Avery Point (Groton, CT, USA) for isotope ratio analyses.

Coral skeletons from specimens collected at Friday Harbor were separated from the coral soft tissue and were rinsed and individually and ultrasonicated two times in Milli-Q™ (MQ) water for 20 minutes each in order to remove any residual seawater. Samples were then individually ultrasonicated in a 1% sodium hypochlorite (bleach) solution for at least two 20-minute intervals with fresh bleach for each new ultrasonication interval until no tissue remained on the skeleton, as assessed visually under a dissection microscope. Individual skeletons were then rinsed and ultrasonicated for 20 minutes in MQ another three times (each time with a new batch of MQ water) in order to remove any bleach residue. Skeleton samples were sent to Pomona College (California, USA) for further processing.

It is necessary to isolate organic matter from the coral carbonate matrix in advance of the N isotope measurement methods used here (see Section 2.6 below). Organic material in the skeleton matrix was isolated and oxidized to nitrate following the protocol of Wang et al. (2014). Briefly, bulk samples weighing 50-100 mg were ground into coarse powder, and a fraction between 63 and 200 μm was collected by sieving through two metal sieves. The 10-15 mg of sieved powder was rinsed sequentially with of sodium polyphosphate-sodium bicarbonate buffered dithionite-citrate reagent, then treated with 13.5% sodium hypochlorite overnight on a shaker. Skeletal material was dissolved in 4 N ultrapure hydrochloric acid, then oxidized to nitrate by autoclaving in basic potassium persulfate solution. Standards of glutamine reference material USGS-40 and USGS-41 (respective $\delta^{15}N$ of 4.52 ‰ vs. air and 47.57 ‰ vs. air) were oxidized in tandem and used to correct for processing blanks. The resulting nitrate samples were sent to the University of Connecticut for nitrate isotope ratio analysis. The long-term averaged reagent blank was 0.4-0.6 μmol L^{-1}, while the typical samples were 10-15 μmol L^{-1} (typical amount of nitrogen in skeleton being 2-5 μmole/g of aragonite). Samples were typically run in duplicates with an average reproducibility of ~ ± 0.5 ‰. An internal laboratory standard of ground material of the cold-water colonial scleractinian coral *Lophelia pertusa* had a long-term $\delta^{15}N$ value 9.4 ± 0.8 ‰ (n=57)

2.5 Hydrographic data

To infer the natural food source of the *B. elegans*, we collected samples for analysis of the $\delta^{15}N$ of particulate and dissolved N pools in relation to ambient hydrographic variables (temperature and salinity) near Friday

248   Harbor, WA. Seasonal sampling campaigns were conducted in September and November 2020 and in April,

249   June, and August 2021 (Table S1). In all but the August 2021 campaign, particulate and dissolved N samples

250   were collected by divers at unspecified depths between the surface and the depth of coral collection. Samples

251   were stored frozen in 30 mL HDPE bottles. Surface net tows were performed with a mesh size of 120 μm;

252   materials were stored and shipped frozen and thawed at a later time to be filtered onto pre-combusted GF/F filters

253   (0.7μm nominal pore size) that were stored frozen pending isotope analysis. No hydrographic variables were

254   recorded during the campaigns except in August 2021.

255   During the August 2021 campaign, depth profiles of temperature and salinity from the surface to 35 m were

256   characterized with a CastAway®-CTD (conductivity temperature depth) profiler. Water samples were collected

257   at 5 m intervals between 5 and 30 m using a Van Dorn water sampler. Water was filtered onto pre-combusted

258   glass fiber filters (GF/F; 0.7μm nominal pore size) into pre-cleaned 30 mL HDPE bottles and stored frozen

259   pending analyses of nitrate concentrations and nitrate isotope ratios. The corresponding filters were stored frozen

260   for isotope ratio analysis of suspended particulate organic material (SPOM). Surface (5 m) and deeper (25 m to

261   the surface) net tows were conducted using plankton nets with respective mesh sizes of 150 μm and 80 μm. Net

262   tow material was filtered directly onto a pre-combusted GF/F filters and frozen pending analysis. A portion of the

263   net tow material from the August 2021 campaign was sieved to separate size classes of 80-100 μm, 100-250 μm,

264   ≥ 250μm, 250-500 μm, and ≥ 500 μm. Material from the respective size classes was filtered onto pre-combusted

265   GF/F filters and frozen until isotope analysis.

266   2.6   Nitrate concentrations and isotope ratio analyses

267   Nitrate concentrations of oxidized coral skeletons and in aqueous samples were measured by reduction to

268   nitric oxide in hot vanadium III solution followed by chemiluminescence detection of nitric oxide (Braman and

269   Hendrix, 1989) on a Teledyne chemiluminescence NOx analyzer Model T200 (Thousand Oaks, CA).

270   The δ^{15}N and δ^{13}C of lyophilized coral tissue samples were analyzed at the University of Connecticut on a

271   Costech Elemental Analyzer–Isotope Ratio Mass Spectrometer (Delta V) and are expressed in standard delta

272   notation (e.g. for N, δ^{15}N (‰ $vs.$ air) = $[[(^{15}N/^{14}N_{sample})/(^{15}N/^{14}N_{air})] - 1]*1000$). Approximately 0.75 mg of

273   lyophilized sample (35 μg N) was allotted into tin cups and analyzed in tandem with recognized glutamine

274   reference materials USGS-40 and USGS-41 with respective δ^{15}N ($vs.$ air) of 4.52 ‰ and 47.57 ‰ and δ^{13}C of -

275   26.39 ‰ and 37.63 ‰ ($vs.$ PDB). Replicate analyses of (n $\geq$ 2) reference materials yielded an analytical precision

276   of (± 1 SD) of 0.3 ‰ for both δ^{15}N and δ^{13}C.

277   Nitrate N (and O) isotope ratios of aqueous seawater samples and N isotope ratios of the skeleton matrix

278   samples were analyzed at University of Connecticut using the denitrifier method (Casciotti et al., 2002; McIlvin

279   and Casciotti, 2011; Sigman et al., 2001). Nitrate sample solutions were injected at target concentrations of 20

280   nmol for seawater samples and 7 nmol for skeleton matrix samples. N_2O was extracted, concentrated and purified

281   using a custom-modified Thermo Gas Bench II equipped with a GC Pal autosampler and dual cold traps and

282   analyzed on a Thermo Delta V Advantage continuous flow isotope ratio mass spectrometer (Casciotti et al., 2002;

283   McIlvin and Casciotti, 2011). Individual analyses were referenced to injections of N_2O from a pure gas cylinder

284   and standardized through comparison potassium nitrate reference materials International Atomic Energy Agency

285   nitrate (IAEA-N3) and the isotopic nitrate reference material United States Geological Survey 34 (USGS-34),

286   with respective $\delta^{15}N$ *vs.* air of 4.7 ‰ and -1.8 ‰ vs. air (International Atomic Energy Agency, 1995), and

287   respective $\delta^{18}O$ of 25.61 ‰ and -27.9 ‰ vs. Vienna Standard Mean Ocean Water (VSMOW; Gonfiantini, 1995;

288   Böhlke et al., 2003). To account for bacterial blanks and source linearity, nitrate concentrations of the standard

289   material – diluted in N-free seawater for aqueous seawater samples and air-equilibrated milli-Q water for

290   skeleton matrix samples – were matched to those of samples within batch analyses, and additional bacterial

291   blanks were also measured (Weigand et al., 2016; Zhou et al., 2022). Replicate measurements ($n \geq 2$) of all

292   samples yielded an average analytical precision (± 1 SD) of 0.3‰ for both $\delta^{15}N$ and $\delta^{18}O$.

293

294   2.7. N turnover model

295   We estimate values of the trophic $\delta^{15}N$ offset for *B. elegans*, ϵ, and the rate of isotopic turnover by fitting

296   the data from our trophic isotope experiment to a nonlinear least-squares regression model corresponding to the

297   isotope mixing relationship shown in Equation 1 below. Equation 1 treats the coral tissue as a single reservoir of

298   N with some initial isotope composition that is evolving to reflect the new diet as a function of time (after Cerling

299   et al. 2007; Ayliffe et al. 2004).

300        $$\delta^{15}N(t) = [\delta^{15}N_{t=0} - \delta^{15}N_{diet} + \epsilon] \cdot e^{-\lambda t} + \delta^{15}N_{diet} + \epsilon. \qquad\qquad \text{Equation 1}$$

301   The term $\delta^{15}N_{t=0}$ is the value of the bulk coral tissue at the onset of the experiment, $\delta^{15}N_{diet}$ is that of the corals'

302   new *Artemia* diet (i.e. what it is fed during the experiment), *t* is the number of days since the start of the

303   experiment, ϵ is the difference between the $\delta^{15}N$ of the diet and tissue at equilibrium (i.e. once the isotopic

304   composition of inputs to the system equals the isotope composition of outputs), and λ describes the specific rate

305   at which new N is incorporated into the coral tissue (days^{-1}). We use this model to calculate the e-folding time of

306 the system, which is defined as $1/\lambda$ (days) and represents the time at which ~63% of the original N reservoir in

307 coral tissue has been replaced with new N from the experimental coral diet.

308

3. Results

310 3.1 Trophic isotope effect

311   At the onset of the culture experiment, the soft tissue among all experimental corals had a δ^{15}N of 11.7 ± 0.5

312 ‰. Over the course of the experiment, the δ^{15}N of the tissue increased or decreased in respective treatments

313 depending on the δ^{15}N of their *Artemia* diet (Figure 3); the tissue δ^{15}N increased in corals fed diets with δ^{15}N

314 values of 17.0, 13.8, and 9.9 ‰, whereas the tissue δ^{15}N decreased for the diet of 6.4 ‰. The δ^{15}N of soft tissue

315 in all groups trended towards an asymptotic offset relative to the diet δ^{15}N, as expected for an approach to a new

316 equilibrium. However, at day 530, at the end of the experiment, it appeared as though the coral tissue δ^{15}N had

317 not yet reached a constant offset value, suggesting that the coral tissue had not yet reached an equilibrium with
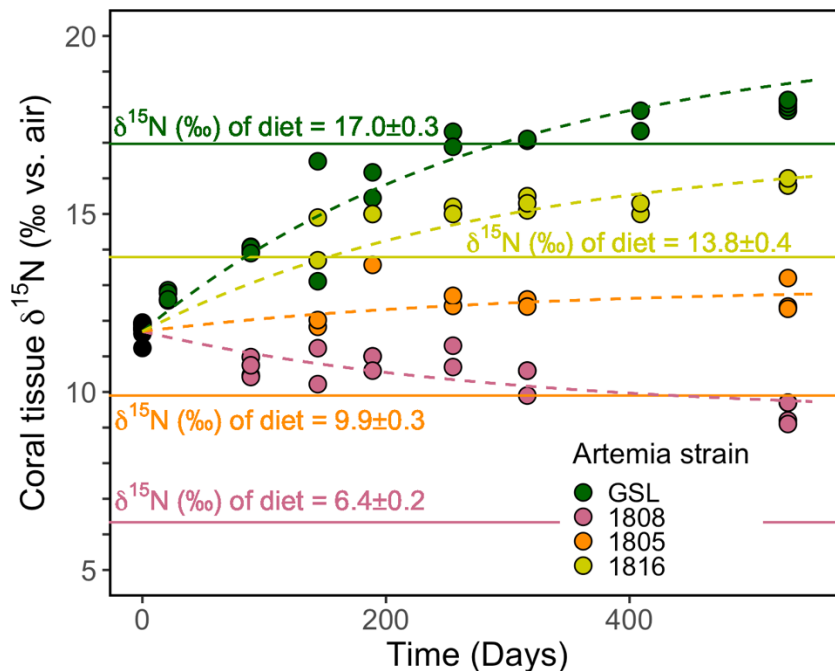
Figure 3. Evolution of the coral soft tissue δ^{15}N in response to diet δ^{15}N. Colors correspond to the respective *Artemia* strains. Dashed lines are the model output of our simultaneous nonlinear least squares regression fits to the data using Equation 1. Solid lines mark the diet δ^{15}N $\pm \sigma$. The mean analytical error on tissue δ^{15}N analyses was ± 0.2 ‰.

318   the new diet. Specifically, at the end of the experiment, the coral tissue of the treatment groups reached $\delta^{15}N$

319   values of 9.4 ± 0.3‰, 12.6 ± 0.5‰, 15.9 ± 0.1 ‰, and 18.1 ± 0.1 ‰ for groups fed the lowest to highest *Artemia*

320   $\delta^{15}N$ values, respectively. The difference between coral soft tissue and diet $\delta^{15}N$ ranged from a minimum of $1.0 \pm$

321   0.1‰ to a maximum of 3.0 ± 0.3‰ across the different experimental groups at day 530 (Figure 3).

322   Despite the fact that coral tissue had not yet reached an equilibrium with the new coral diet at the end of our

323   experiment, we are able to estimate values of the trophic $\delta^{15}N$ offset for *B. elegans*, ϵ, and the rate of isotopic

324   turnover by fitting the data from our trophic isotope experiment to the nonlinear least-squares regression model

325   given Equation 1 in Section 2.7. To more confidently calculate ϵ and λ for each individual experimental group,

326   we generate 4 equations, (one for each experimental group of the form given in Eq. 1 but with different values of

327   $\delta^{15}N_{diet}$) and fit them simultaneously using least-squares regression. From this fit, we are able to obtain estimates

328   for both ϵ and λ in *B. elegans*. An inherent assumption of this approach is that all experimental groups have the

329   same e-folding time and the same trophic isotope effect. We note here that we refer to the e-folding time as the

330   'turnover rate' of N in corals throughout the rest of this text (e.g., Tanaka et al. 2018). Our model fit yielded a

331   trophic isotope effect, ϵ, of 3.0 ‰ with a standard error of 0.1 ‰ between coral tissue and diet. The turnover rate

332   of N (i.e. e-folding time, $1/\lambda$) was 291 days with a standard error of 15 days. The four individual model equations

333   generated by our nonlinear least squares regression are presented as the dashed lines in Figure 3.

334   3.2 Effect of starvation

335   At the onset of the starvation trial, the coral tissue had an average $\delta^{15}N$ of 11.5 ± 0.1 ‰. At the end of the

336   522-day experiment, the starved group (N=15 coral individuals) had an average $\delta^{15}N$ of 12.4 ± 0.4 ‰ and the

337   frequently fed group (N=15) with a $\delta^{15}N$ of 12.7 ± 0.1 ‰ (Figure 4). The starved group was $+2.5 \pm 0.4$ ‰

338   compared to its diet, statistically indistinguishable from that of the frequently fed group of +2.8 ± 0.1 ‰ higher

339   than the diet (p-value = 0.059, pairwise t-test).
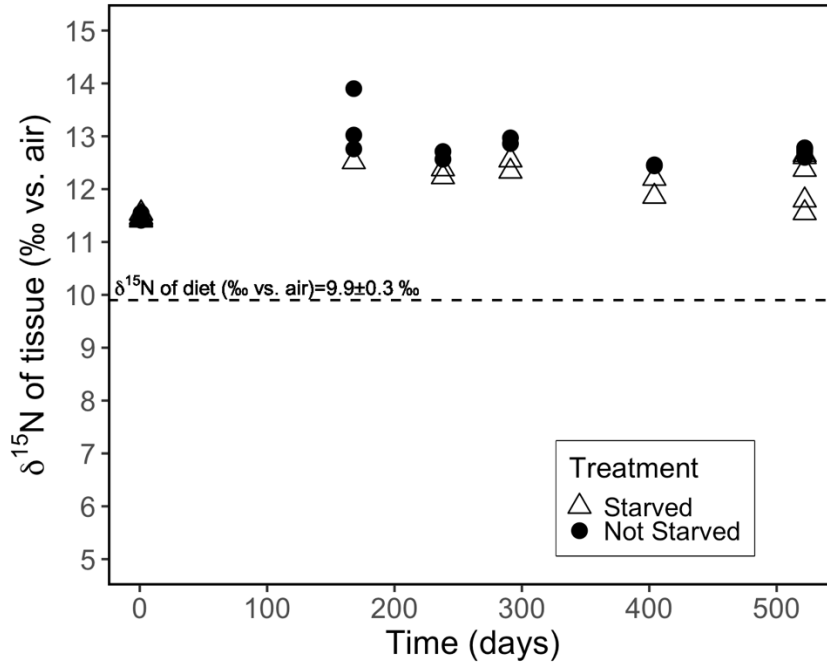
Figure 4. Evolution of the δ^{15}N of individual coral polyps fed *Artemia* nauplii (δ^{15}N 9.9 ‰) twice weekly (not starved) *vs.* every two weeks (starved). The analytical error associated with individual tissue δ^{15}N measurements was ± 0.2 ‰.

340   3.3 δ^{15}N comparison of field specimen polyp tissue and skeleton

341   The δ^{15}N of the soft tissue from individual *B. elegans* specimens collected live near Friday Harbor ranged

342   between 11.2 to 13.1 ‰, averaging 12.0 ± 0.6 ‰ (Figure 5a). The soft tissue δ^{15}N differed among coral groups

343   collected during different sampling campaigns, with higher values in spring (March 2019 and April 2021)

344   compared to summer and fall (June 2019, September and November 2020; ANOVA F(4) = 40.39; p-value ≤ 0.01,

345   post-hoc pairwise t-test; p-value < 0.05). The average δ^{15}N of corresponding skeletal tissue was 13.5 ± 0.7 ‰ and

346   did not differ discernibly among sampling campaigns (ANOVA F(2) = 0.916; p-value = 0.431). The average

347 difference between skeleton and soft tissue $\delta^{15}N$ ($\Delta\delta^{15}N$) among coral individuals for which both soft tissue and

348 skeleton was measured was 1.2 ± 0.6 ‰ (Figure 5b).
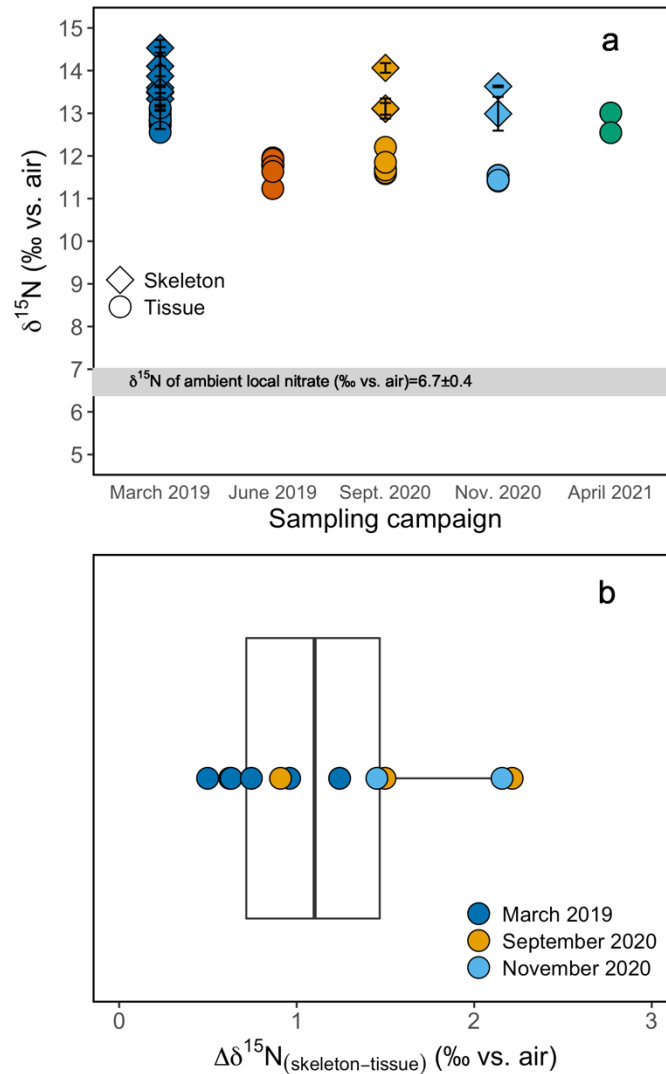
Figure 5. (a) Tissue and skeleton $\delta^{15}N$ measurements from *B. elegans* individuals collected during different sampling campaigns. Errors on skeleton data are based on replicate analyses of samples from individual polyps. (b) Boxplot of the difference between tissue and skeleton of individual *B. elegans* corals. The boxplot shows the mean, first and third quartile, maxima, and minima. Individual data points are overlaid on the plot. Colors correspond to respective sampling campaigns.

349 3.4 Regional hydrography and N isotope ratios of nitrate and plankton material

350   Hydrographic profiles recorded at stations near Friday Harbor in August 2021 showed characteristic density

351 structures that were sensitive to tidal phase (Figure 6 a,b; Banas et al. 1999). Profiles collected during flood tide

352 (collected between 11:40 and 14:20 on August 2, 2021) were relatively well-mixed (salinity 30, temperature

353 11.8°C), with fresher and warmer water restricted to the near surface (≤ 5 m), whereas ebb-tide profiles (collected

354 at 9:00 on August 2, 2023) showed a progressive decrease in salinity from 30 to 27 and a corresponding increase

355 in temperature from 11.8°C at 35 m to 14.5°C at the surface.

356 Nitrate concentrations were nearly uniform with depth during flood tide (~20 µmol L^{-1}), decreasing slightly at

357 5 m, whereas during ebb tide nitrate concentrations decreased progressively from 20 to 10 µmol L^{-1} between 30

358 and 10 m (Figure 6c). Nitrate concentrations in samples collected during the other sampling campaigns ranged

359 from 12 to 32 µmol L^{-1}, and appeared generally higher at stations visited during the September and November

360 2020 campaigns compared to those in April and August 2021 (Figure S6).

361 Depth profiles collected in August 2021 revealed uniform nitrate δ^{15}N values of ~7 ‰ at 30 m among

362 profiles. In well-mixed profiles, nitrate δ^{15}N increased slightly to 7.5 ‰ above 10 m. In stratified profile, nitrate

363 δ^{15}N increased progressively to 8.2 ‰ at 10 m (Figure 6d). Among all sampling campaigns, the δ^{15}N of nitrate

364 ranged from 6.1 ‰ to 8.2 ‰, with median values of 6.8 ± 0.4 ‰ (Figure 7a). The relationship between nitrate

365 δ^{15}N and nitrate concentration in August 2021 was fit to a closed-system Rayleigh distillation model (Mariotti et

366 al. 1981), suggesting a nitrate assimilation isotope effect of 1.5 ± 0.1 ‰ (Figure 8).
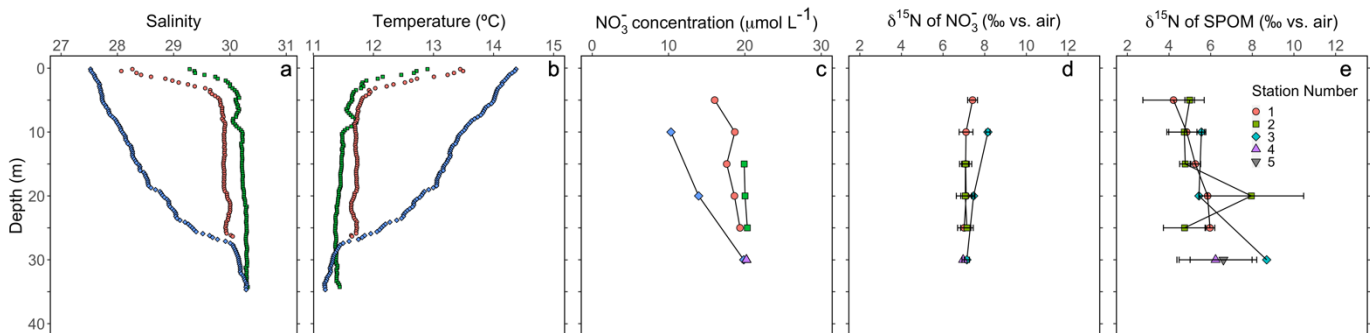
Figure 6. Depth profiles during the August 2021 sampling campaign of (a) salinity, (b) temperature, (c) nitrate concentration, (d) the δ^{15}N of nitrate for analytical replicates and (e) the δ^{15}N of SPOM of replicate samples (n ≥ 2). Green and red symbols correspond to flood tide (collected between 11:00am and 2:00pm on August 2, 2021), blue symbols correspond to ebb tide (collected at 9:00am on August 3, 2021).

367 The δ^{15}N of SPOM collected at depths above 35 m near Friday Harbor during the different sampling

368 campaigns ranged from 1.6 to 11.7 ‰, averaging 5.7 ± 1.7 ‰ (Figure 7b). Values were lowest for the four

369 samples collected in April (4.4 ± 0.4 ‰), and highest for the four samples collected in September and November

370 (6.2 ± 2.6 ‰), although these trends may be an artifact of the low data density in April (n = 4) and Sept./Nov. (n

371 = 5) relative to August 2021 (n = 29), at which time the observed range of δ^{15}N subsumed that in the other two

372 campaigns. Values did not differ coherently with depth in August 2021, although any potential depth structure

373 was obscured by the large variability among sample replicates (Figure 6e).
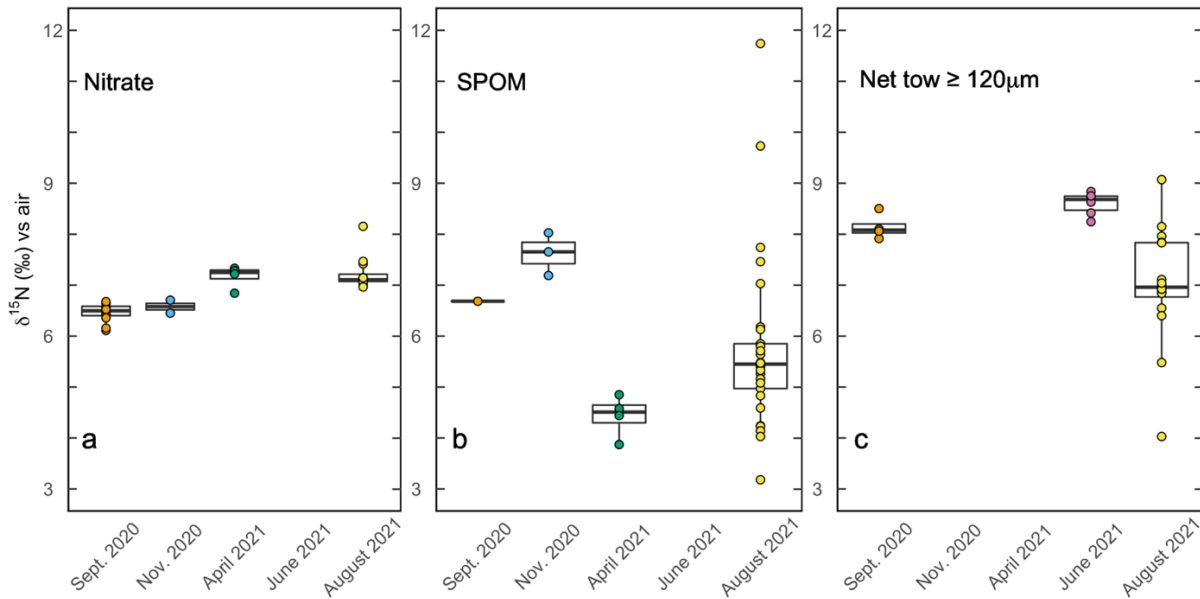
Figure 7. Boxplots of aqueous and particulate N pools at respective sampling times. (a) The $\delta^{15}N$ of nitrate from samples above 30 m collected during respective sampling campaigns. (b) The $\delta^{15}N$ of suspended particulate organic matter (SPOM) at sites near Friday Harbor during respective sampling campaigns. (c) The $\delta^{15}N$ of net tows ($\geq$ 120 μm mesh size) conducted during respective sampling campaigns.

374 The $\delta^{15}N$ of material collected in net tows (120 μm mesh size) during sampling campaigns in September 2020,

375 and June 2021 ranged between 7.9 to 8.8 ‰ (Figure 7c). Material collected in net tows of 80 μm and 150 μm

376 mesh size in August 2021 and separated by size class post-collection revealed a coherent $\delta^{15}N$ increase with size

377 class (Figure 7c; Figure 9). The $\geq$ 80 μm size class had a mean $\delta^{15}N$ of 6.0 ± 0.3 ‰ whereas that $\geq$ 500 μm had an

378 average $\delta^{15}N$ of 8.0 ± 0.8 ‰, which was significantly greater than the $\delta^{15}N$ of the other size classes (ANOVA, p-

379 value <0.05).

4. Discussion

381 This study of *B. elegans* provides novel constraints on the trophic ecology of scleractinian CWCs. Foremost,

382 our observations of *B. elegans* collectively suggest that the relatively large global $\delta^{15}N$ offset of 8-9 ‰ between

383 CWC skeletal tissue and the $\delta^{15}N$ of PON exported from the surface ocean is neither explained by a large

384 difference between tissue and skeleton $\delta^{15}N$, nor by an unusually large trophic isotope effect. Further, controlled

385 feeding experiments yielded direct estimates of the trophic isotope effect and the corresponding N turnover rate

386 of *B. elegans* soft tissue. Examination of soft tissue $\delta^{15}N$ of wild specimens in relation to regional hydrography

387 and food web components near Friday Harbor leads us to conclude that *B. elegans* feeds predominantly metazoan

388 zooplankton prey, implicating more than one trophic transfer between exported PON and coral soft tissue. We

389 contextualize our findings to existing studies of CWC trophic ecology and discuss the implications of considering

390 a two-level trophic transfer for paleo-reconstructions of ocean N cycling using *B. elegans* and CWCs more

391 generally.
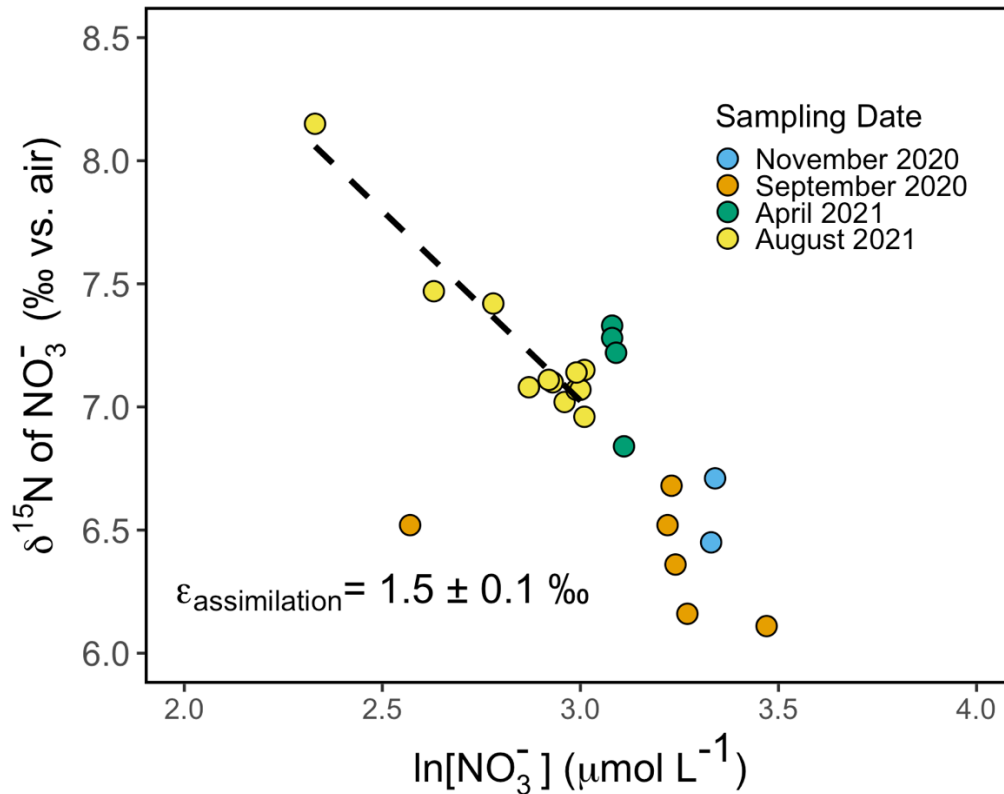
Figure 8. Rayleigh plot of nitrate $\delta^{15}N$ vs. ln of nitrate concentration for samples collected from the surface to 40 m around Friday Harbor. The isotope effect of ~1.5 ± 0.1 ‰ corresponds to the slope of the best fit linear regression line for the August 2021 data, $\delta^{15}N_{NO3} = 11.7 - 1.5 \ln [NO_3^-]$.

392 4.1 Culture experiments revealed a normal trophic isotope effect

393   We investigated whether the large difference in $\delta^{15}N$ between PON export from the surface and coral

394 skeleton-bound $\delta^{15}N$ (8-9 ‰) observed by Wang et al. (2014) could arise from an unusually large trophic level

395 offset specific to CWCs. The long-term feeding experiment of *B. elegans* polyps revealed a 'normal' trophic

396 isotopic offset between coral tissue and diet of ε = +3.0 ± 0.1 ‰. This value conforms to the expected range of
397 +3.4 ± 1.1 ‰ for a single trophic level offset in δ^{15}N (Minagawa and Wada, 1984).

398
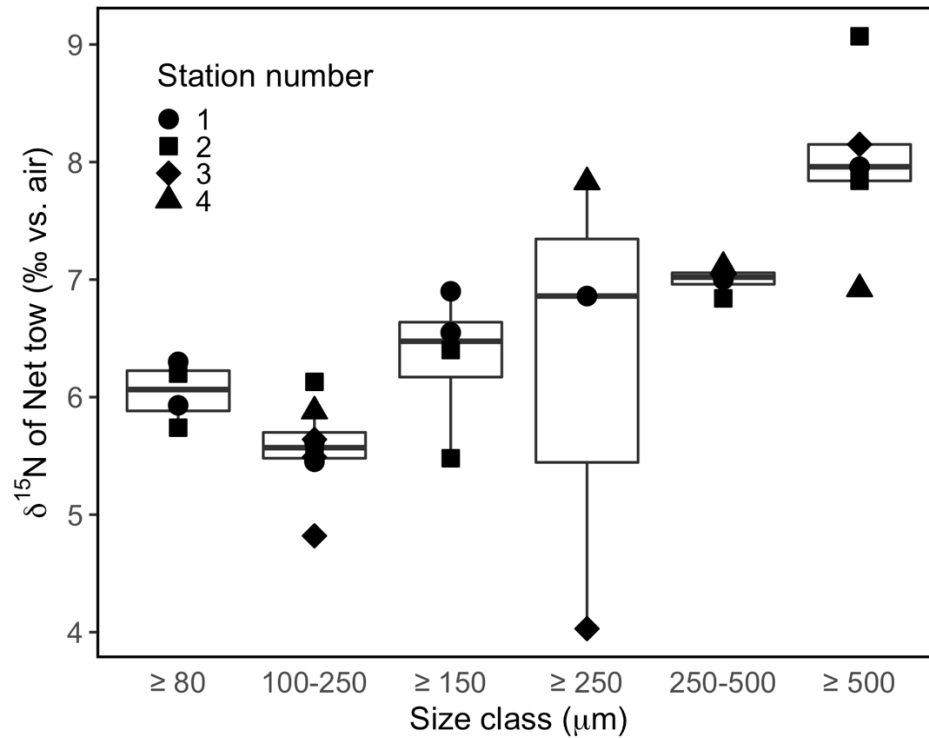
Figure 9. Boxplots of net tow material collected above 30 m in August 2021, separated by size class.

399

400   To support the above conclusion, we assess the assumptions inherent to the isotope mixing model (Eq. 1)
401 used to derive ε and the corresponding nitrogen turnover rate from our culture data. First, the model only
402 accounts for the turnover of a single pool of N, requiring the assumption that all N in the coral polyp tissues
403 equilibrate at the same rate. This notion is unlikely to be wholly accurate, as fluxes of N may vary among tissue
404 types. However, given the relatively low resolution of our sampling over the course of the culture experiments
405 (necessary due to constraints on numbers of total samples) we are unable to extend our model to one with
406 multiple pools (*e.g.* as in Ayliffe et al. 2004). As soft tissues of individual coral polyps were homogenized, we
407 suggest that the δ^{15}N values and corresponding estimate of ε thus represent the average of soft tissues with
408 potentially different turnover rates. The estimates of ε and N turnover rate further rely on the assumption that the

409   nutritional quality of the respective diets among treatments was equivalent, as trophic isotope effects can be

410   sensitive to food type. Diets low in protein can be associated with greater ε values due to internal recycling of

411   nitrogen (Adams and Sterner, 2000; Webb et al., 1998). For instance, locusts fed a low protein diet were enriched

412   5.1 ‰ from their diet, compared to 2.3‰ for those fed a high protein diet (Webb et al., 1998). Conversely, a

413   compilation of studies of various metazoan consumers raised on controlled diets suggests that high protein diets

414   generally result in higher trophic isotope effects (~3.3 ‰) compared to more herbivorous diets (~2.2 ‰), a

415   dynamic ascribed to higher rates of N excretion to assimilation in consumers fed high protein diets (McCutchan

416   Jr et al., 2003). As noted in Table S3 and in Section 2.3.1, our *Artemia* prey had similar C:N ratios among

417   treatments, in line with our model treatment. Finally, our model assumes that N turnover was dominated by

418   metabolic tissue replacement, rather than net growth, consistent with the observation that adult *B. elegans* growth

419   is slow (Gerrodette 1981).

420   Equation 1 could be invalidated if the corals can access nutritional N sources other than N in *Artemia*, given

421   that the model assumes that *Artemia* are the only source of N to corals in our experiment. Biological N_2 fixation

422   and chemoautotrophy have been detected in association with CWC holobionts, providing some N nutrition to the

423   corals (Middelburg et al., 2016). Our trophic isotope effect estimate was in the range expected for a single trophic

424   transfer, arguably suggesting that N_2 fixation, if occurring, was not a substantial contribution to the corals'

425   nutrition; it would otherwise result in a lower value of ε given a $\delta^{15}N$ contribution of -1 to 0 ‰ (Carpenter et al.

426   1997). That the trophic isotope effect of the poorly fed corals did not differ from that of corals that were well-fed

427   also argues for no sources of N additional to the *Artemia*, as starved corals would presumably increase their

428   reliance on said source. In a related vein, N recycling between the *B. elegans* specimens and potential microbial

429   symbionts (e.g. Middelburg et al. 2016) could also dampen the trophic isotope effect relative to the *Artemia* prey

430   and yield an over-estimate of soft tissue turnover rate for N. The normal trophic isotope effect indicated here

431   suggests a modest role of N retention and recycling by microbial symbionts, in contrast to tropical symbiotic

432   corals wherein bacterial symbionts promote substantial N retention and recycling, and consequently lower trophic

433   isotope effects (Tanaka et al. 2018). Finally, the validity of our estimates could be sensitive to differences in

434   feeding rates, which can influence the rate of N turnover of tissues (Martínez del Rio and Carleton, 2012; Rangel

435   et al., 2019). Corals were fed at identical times among treatments, at a relatively high feeding rate (Crook et al.,

436   2013). However, given the limited number of studies on feeding in *B. elegans*, it is difficult to compare our

437   feeding strategy and that of this species' natural environment. Overall, we consider that the mixing model

438 described by Equation 1 is appropriate to derive the first-order trophic isotope effect and turnover rate of *B.*
439 *elegans*.

440   Changes in metabolism due to underfeeding or prolonged fasting have the potential to increase trophic-level
441 isotope offsets due to increased protein metabolism (Adams and Sterner, 2000). For instance, extensive amino
442 acid recycling in overwintered adult insect larvae was cited to explain trophic isotope effects upward of 10‰
443 (Scrimgeour et al., 1995). A meta-analysis on the effects of starvation on consumer δ^{15}N revealed that starvation
444 generally led to increased organism δ^{15}N by an average of 0.5 ‰, up to 4.3 ‰ (Doi et al., 2017). This dynamic
445 was documented for the tropical symbiotic coral *Stylophora phistillata*, where heterotrophically starved corals
446 were enriched in δ^{15}N by ~0.5 ‰ compared to frequently fed corals (Reynaud et al., 2009). The trophic isotope
447 offset of *B. elegans* soft tissue relative to its diet, ε, was not discernibly influenced by near starvation; that of
448 corals fed once every other week was similar to that of corals fed twice a week – in spite of visible signs of stress
449 among the former, including relatively more sluggish feeding (Figure S7) and thinner soft tissue (data not
450 shown). Deep sea coral reefs are often highly productive environments with high levels of biodiversity,
451 commensurate with a relatively high food supply (Duineveld et al., 2007; 2004; Genin et al., 1986; Roberts et al.,
452 2006; Soetaert et al., 2016; Thiem et al., 2006; Cathalot et al. 2015). Nevertheless, periodicity and spatial
453 heterogeneity in the food supply of CWC reefs implicate periods of lower food density (e.g., Duineveld et al.
454 2007). High currents, downwelling and/or vertically migrating zooplankton temporally boost the export of
455 surface organic matter to the seabed, creating 'feast' conditions, interspersed with 'famine' periods during the
456 non-productive season (Maier et al. 2023). Regardless, our trials suggest that starvation, if pertinent to CWC
457 communities, does not result in greater-than-expected trophic isotope offsets, at least for *B. elegans*.

4.2 Turnover rate for *B. elegans*

459   We report the first estimate of the nitrogen turnover for a non-symbiotic cold-water coral of 291 ± 15 days
460 for *B. elegans* soft tissue. This value falls within the range of existing estimates for tropical symbiotic corals.
461 Pulse-chase experiments with ^{15}N-nitrate conducted with fragments of the tropical symbiotic coral *Porites*
462 *cylindrica* yielded a N turnover time of 370 days, and of 210 days for the tropical symbiotic coral *Acropora*
463 *pulcra* (Tanaka et al. 2006; 2018). These relatively long turnover times are attributed to the recycling and
464 retention of N within the coral-symbiont system in nutrient-deplete ecosystems. In comparison, the corresponding
465 carbon turnover in *A. pulcra* was 18 days – compared to 210 days for N – because the system is ultimately N
466 limited (Tanaka et al., 2006). Tanaka et al. (2018) inferred that the N turnover in *P. cylindrica* would be
467 substantially faster than 370 days without symbionts, on the order of 56 days based on estimates of polyp-specific

N uptake rates. Nevertheless, the N turnover estimated for the tropical symbiotic coral *Porites lutea* was notably shorter that *A. pulcra and P. cylindrica*, on the order of 87 days (Rangel et al., 2019), implicating different N nutritional strategies among symbiotic coral groups and/or ecosystems. The N turnover for *B. elegans* estimated here is of the same order as but still longer than that for tropical symbiotic corals suggesting that cold-water species have lower metabolic and growth rates compared to tropical symbiotic species, although efficient N recycling has also been documented previously in cold-water corals (Middelburg et al. 2016). The slower turnover of CWCs relative to their symbiotic tropical counterparts may reflect the lower temperatures of the former's habitats (Miller, 1995; Thomas and Crowther 2015).

Constraints on N turnover also allow for calibration of the temporal resolution that is achievable with the CWCs δ^{15}N proxy for marine N cycling. Corals are constantly accreting skeleton, such that coral proxies have the potential to provide annual resolution (*e.g.*, Adkins et al. 2004). In theory, a rapid N turnover in CWC could record seasonal changes in regional N dynamics. A turnover time of 291 ± 15 days for N in *B. elegans* soft tissue, however, signifies that the δ^{15}N of coral skeleton is unlikely to provide a faithful record of seasonal differences in the δ^{15}N of the coral diet. Moreover, the turnover of the pool of N that sources the skeletal tissue may be different from that of bulk tissue, and thus decoupled from the soft tissue turnover rate. We suggest that CWCs can likely record changes in their diet on annual or longer timescales, compatible with the ability to date CWC with subdecadal resolution (Adkins et al. 2004).

4.3 Soft tissue vs. skeleton δ^{15}N

A large biosynthetic δ^{15}N offset between the coral soft tissue and its skeleton could conceivably account for a large δ^{15}N offset between coral skeleton-bound organic matter and N of export that is not explained by single trophic level enrichment of ~3 ‰. However, the mean difference between soft tissue and skeleton-bound δ^{15}N among *B. elegans* specimens collected at Friday Harbor was relatively modest, on the order of +1.2 ‰, ranging between +0.5 and +2.2 ‰. The observed range was dictated primarily by the variability in the δ^{15}N of the coral soft tissue, as skeleton-associated δ^{15}N values were relatively invariant among specimens sampled from different locations and field seasons – likely due to the fact that the amount of skeleton analyzed represented multiple years of growth. The amount of skeleton-bound organic N is small relative to aragonite mass (2-5 µmol N per g of skeleton in our samples), such that homogenization of 50-100 mg aragonite fragments may alias seasonally-driven variability in skeletal δ^{15}N. Soft tissue values in spring were ~1.5 ‰ higher than in summer and fall, such that they appeared to record seasonal changes in diet (Figure 5a). In this regard, the asymptotic nature of the two end-member isotope mixing model (Eq. 1) renders *B. elegans*'s soft tissue sensitive to seasonal changes in prey

498   δ^{15}N, but not likely to reach isotopic equilibrium on seasonal timescales - given an N turnover of ~291 days, as

499   discussed above. Seasonal variations in the δ^{15}N of the food source of *B. elegans* near Friday Harbor could arise

500   from corresponding differences in the δ^{15}N of nitrate entrained to the surface driven by seasonal hydrographic

501   variability around San Juan archipelago, in the extent of surface nitrate consumption, in food web structure, or

502   from some combination of these. The data density among all but the August 2021 sampling campaign is too

503   sparse to be conclusive in this regard. Otherwise, the observed differences in soft tissue δ^{15}N may result from

504   spatial heterogeneity in food source δ^{15}N among the different collection sites visited for respective campaigns at

505   Friday Harbor.

506   As documented here for *B. elegans*, the δ^{15}N difference between coral tissue and skeleton appears to be

507   modest among various scleractinian coral species. Specimens of the symbiotic tropical coral *Porites lutea* showed

508   a δ^{15}N offset of +1.1 ‰ between skeleton and soft tissue, whereas the symbiotic tropical coral *Favia stelligera*

509   revealed an insignificant offset of -0.1 ‰ (Erler et al., 2015). Similarly, no offset was observed for proteinaceous

510   cold-water corals of the genus *Lepidisis* collected off Tasmania (Sherwood et al., 2009), whereas an offset of -1.9

511   ± 0.8 ‰, was reported for cold-water proteinaceous corals of the genus *Primnoa* from the Gulf of Alaska,

512   *Isadella* from the Central California Margin, and *Kulamanamana* from the North Pacific Subtropical Gyre

513   (McMahon et al., 2018). Conversely, a study of numerous species of both symbiotic and non-symbiotic corals

514   reported a +4 ‰ offset between the skeletal organic matrix and soft tissue among the non-symbiotic corals

515   specifically, but no difference among the symbiotic corals (Muscatine et al., 2005), suggesting that biosynthetic

516   offsets may occur for certain CWC species or conditions.

517   4.4   Implications for components of CWC diet

518   Cold water corals are considered opportunistic feeders, ingesting whatever is available in the water column

519   (Mortensen, 2001; Freiwald, 2002; Duineveld et al. 2004; 2007; Kiriakoulakis et al. 2005; Carlier et al. 2009;

520   Dodds et al. 2009; van Oevelen et al. 2009). They are reported to feed on zooplankton (Kiriakoulakis et al., 2005;

521   Naumann et al., 2011), including microzooplankton (Houlbrèque et al. 2004), on phytoplankton and

522   phytodetritus, including the bacterial fraction of phytodetritus (Maier et al., 2020; Houlbrèque et al. 2004),

523   dissolved organic matter (Mueller et al., 2014; Ferrier 1991, Al-Moghrabi et al. 1993; Hoegh-Guldberg &

524   Williamson 1999; Houlbrèque et al. 2004; Grover et al. 2008), and the CWC holobiont has been observed to

525   display biological N_2 fixation and chemoautotrophy (Middelburg et al. 2016). While it is clear that corals may be

526   able to consume a variety of components within the food web, the soft tissue δ^{15}N of *B. elegans* specimens

527   collected at Friday Harbor averaged 12.0 ‰, signifying that they fed on material with a δ^{15}N of approximately

528 9.0 ‰ – accounting for a normal trophic offset relative to their diet (3 ‰) confirmed by our culture experiment

529 results. Here, we seek to determine the primary nutrition source for *B. elegans* at Friday Harbor by comparing the

530 $\delta^{15}N$ of these corals' expected diet with measured $\delta^{15}N$ of different food web components including SPOM and

531 net tow material.

532   We first explore whether the SPOM fraction of the food web was the dominant component of *B. elegans'* diet

533 at Friday Harbor. SPOM is operationally defined as the particulate material retained onto glass fiber filters (GF/F,

534 0.7μm nominal pore size) from filtered aqueous samples. At the ocean surface, including at the stations near

535 Friday Harbor, SPOM is generally dominated by phytoplankton material. At the ocean subsurface, below the

536 euphotic zone, SPOM derives from organic material exiting the ocean surface, but is considered a distinct pool

537 from the ballasted sinking PON collected in sediment traps. The $\delta^{15}N$ of SPOM typically increases with depth,

538 with the steepest gradient across the 100-300 m depth interval, reaching upwards of ~4-5 ‰ in the ocean

539 subsurface, which are higher values than the corresponding sinking particles at abyssal depths due to recycling

540 and remineralization (Altabet, 1988; Casciotti et al., 2008; Saino and Hattori, 1987). Wang et al. (2014) reasoned

541 that because the $\delta^{15}N$ of SPOM is approximately one trophic level lower that of the N preserved in skeletons of

542 the deep-dwelling (deeper than ~ 500 m) CWC *Desmophyllum dianthus,* and because suspended particles are the

543 most abundant form of small particles in the deep ocean, cold-water corals must feed predominantly on SPOM.

544 However, SPOM collected in the upper 30 meters near Friday Harbor was 5.7 ± 1.7 ‰, which is ~ 6 ‰ lower

545 than *B. elegans* soft tissue, a difference greater than expected for a single trophic level. Thus, the SPOM at Friday

546 Harbor was evidently not the predominant food source for *B. elegans* growing in this depth interval.

547   Additionally, it has been suggested that CWCs can assimilate dissolved organic nitrogen (DON) (Gori et al.,

548 2014). We do not have $\delta^{15}N$ DON measurements from our field study. However, we do not expect the potential

549 assimilation of DON to explain the elevated $\delta^{15}N$ of organic tissue that was observed. There are two components

550 of marine DON, refractory and labile (Bronk et al. 2002), which have different $\delta^{15}N$ (Knapp et al. 2018). At

551 Friday Harbor, we don't know the partitioning of the $\delta^{15}N$ between these pools, but even if we did, the labile

552 fraction (which would presumably be the pool available to corals) is expected to converge on the $\delta^{15}N$ value of

553 SPOM (Bronk et al., 2002, Sigman and Fripiat 2019 their Fig. 4; Knapp et al., 2018, Zhang et al., 2020), given

554 that the most recently produced DON is generally most labile. As a result, consumption of DON would not

555 explain the high $\delta^{15}N$ of coral organic tissue.

556   Instead, we suggest that the relatively high $\delta^{15}N$ of ~ 12 ‰ of *B. elegans* soft tissue at Friday Harbor results

557 from these corals deriving nutrition predominantly from larger metazoan zooplankton. Indeed, this is supported

558 by a comparison of the $\delta^{15}N$ coral tissue and the $\delta^{15}N$ of the largest size class of net tow material (≥ 500 μm) of

559 8.0 ± 0.8 ‰. This is the only component of the organic matter nitrogen budget that is offset from the coral tissue

560 by ~ 3.5 ‰, consistent with one trophic level transfer. Additionally, the net tow material had a molar C:N ratio of

561 4.4 ± 0.6, compared to 6.5 ± 2.2 for the SPOM (Figure S8), suggesting a dietary preference for metazoan

562 zooplankton would provide higher protein content and nutritional density for these corals (Adams and Sterner,

563 2000).

564   Despite evidence for zooplankton as the main dietary source for *B. elegans* at Friday Harbor, we

565 acknowledge that this feeding strategy may not apply for corals of other species living in habitats that are

566 hundreds to thousands of meters deep. As pointed out in a recent review (Maier et al. 2023), the presence of

567 CWC reefs in the food-limited deep ocean appears paradoxical, and it is not likely that the food available to

568 corals at Friday Harbor looks identical to food available to corals living at >1000 m water depth. Indeed, Maier et

569 al. 2023 suggest that the biodiversity and productivity of CWC reefs in the deep sea are supported by a number of

570 processes such as CWC's ability to consume a range of dietary components in addition to zooplankton (DOM,

571 bacterioplankton, inorganic resources such and inorganic C and ammonium), efficient resource recycling, and

572 their ability to align their feeding strategies and growth with fluctuations in food availability. For example, it has

573 been suggested that sponges, some of which are known to have high δ^{15}N due to efficient internal recycling,

574 generate dissolved and particulate organic nitrogen that is then transferred to other associated deep-sea organisms

575 such as brittle stars (Hanz et al. 2022; Kahn et al. 2018). At the moment, however, we do not have any evidence

576 that this deep-sea "sponge loop" directly influences the N isotope composition of CWCs. Additionally, while we

577 cannot speculate about the flux of DOM to corals living at >1000m depth, we note that the δ^{15}N of deep DOM

578 has a uniform value of ~5 ‰, which cannot explain the high δ^{15}N of CWCs (see Sigman and Fripiat, 2019).

579   Maier et al. (2023) and references therein highlight that most deep CWC reefs occur in regions with higher-

580 than-average annual primary productivity, indicating that these CWC reefs are sustained by inputs of high energy

581 to the system, where there is also evidence for the presence of vertically migrating zooplankton. The vertically

582 migrating zooplankton have been found near both relatively shallow (<200 m, Duineveld et al. 2007, Garcia-

583 Herrera et al., 2022) and deep (~1000 m, e.g. Carlier et al. 2009) CWC reefs. Moreover, there are a number of

584 other independent studies that reveal a single trophic level offset between the δ^{15}N of zooplankton prey and the

585 δ^{15}N soft tissue of asymbiotic scleractinian corals at specific sites (Duineveld et al., 2004, Sherwood et al. 2005;

586 2008; 2009; Carlier et al., 2009; Hill et al., 2014; Maier et al., 2020). Given the 'normal' trophic level offset

587 reported for CWCs in our laboratory culture experiment, these published observations underscore that

588 zooplankton could be a dominant dietary component of corals other than *B. elegans* as well. Additional evidence

from lipid biomarkers corroborates the assertion that deep-dwelling CWC species such *Lophelia pertusa* (recently re-classified as *Desmophyllum pertusum*) and *Madrepora oculata* feed predominantly on metazoan zooplankton (Dodds et al., 2009; Kiriakoulakis et al., 2005; Naumann et al. 2015). Some deep-dwelling CWCs (*Desmophylum pertusum, Madrepora oculata, Dendrophyllia cornigera*) exhibit prey preference for larger zooplankton (Da Ros et al. 2022), suggesting that zooplankton prey are an essential component of their diet. Indeed, an exclusive diet of phytodetritus (Maier et al. 2019) and the exclusion of zooplankton from diet (Naumann et al. 2011) led to decreases in coral metabolism. More fundamentally, the shared traits of tentacles and nematocysts are evidence of a predatory life strategy, indicating that zooplankton are an important food source for corals (Lewis and Price, 1975; Sebens et al., 1996). The coral morphology of *B. elegans* and that of other cold water scleractinian corals is consistent with an adaptation for the capture of prey of a commensurate size (Fautin, 2009). Correspondingly, *D. dianthus* is considered to be a generalized zooplankton predator that can prey on medium to large copepods and euphasiids (Höfer et al., 2018). In contrast, gorgonian corals do not capture naturally occurring zooplankton and have a correspondingly low density of nematocysts (Lasker 1981). In summary, while our data cannot directly indicate that all CWCs, including the deep-dwelling ones, derive their primary nutrition from zooplankton, the results of our trophic experiment and field study (when evaluated in the context of the published literature) suggest that it may be important to consider metazooplankton as a significant component of CWC diet, and that CWC δ^{15}N is likely to be sensitive to food web dynamics. We discuss the implications of these suggestions further in the sections below.

4.5 Does coral-bound δ^{15}N reflect surface ocean processes at Friday Harbor?

The effectiveness of coral skeleton-bound δ^{15}N as an archive to reconstruct past ocean N cycling depends on its ability to record the δ^{15}N of the surface PON export. In turn, the δ^{15}N imparted to the phytoplankton component of surface particles, from which PON export derives, is highly dependent on surface ocean dynamics that influence the degree of nitrate consumption and associated isotope fractionation. Here, we describe local marine N cycling dynamics in order to evaluate whether coral-bound δ^{15}N recorded in the *B. elegans* specimens reflects local surface ocean processes.

Given complete assimilation of inorganic N pools, the δ^{15}N of phytoplankton material - the dominant component of SPOM at the surface ocean - converges on the δ^{15}N of the N sources, new nitrate and recycled N sources (Treibergs et al., 2014; Fawcett et al. 2011). At steady state, the δ^{15}N of the sinking PON flux reflects the isotope signature of the nitrate upwelled to the surface (Altabet, 1988). Alternatively, given partial nitrate consumption in the context of a finite pool (Rayleigh dynamic), such as in high-nutrient low-chlorophyll regions

and in upwelling systems, the SPOM δ^{15}N is fractionated relative to the nitrate δ^{15}N as function of the assimilation isotope effect and the extent of nitrate consumption (Sigman et al., 1999). The δ^{15}N of the sinking flux then reflects both the δ^{15}N of nitrate upwelled to the surface and the degree of nitrate consumption (Altabet and François 1994; François et al. 1997). In this section, we discuss whether coral-bound δ^{15}N reflects the δ^{15}N of nitrate entrained to the surface.

Nitrate assimilation at Friday Harbor appeared to be incomplete, potentially implicating the fractionation of N isotopes between nitrate and biomass. Although depleted nitrate concentrations are generally expected at coastal sites during the summer in density stratified water column due to phytoplankton assimilation, nitrate concentrations at Friday Harbor in August of 2021 were upwards of 15 µM at the surface and 20 µM at 30 m depth. Indeed, nitrate in the San Juan Channel is replete year-round, even at the surface, due to vigorous mixing within the channel (Mackas and Harrison, 1997; Murray et al., 2015).

The region experiences tidal mixing, designating it as a well-mixed estuary with minimal density stratification (Mackas and Harrison, 1997). The tidal influence is clearly identified from the diurnal patterns of vertical hydrographic structure variability with the salinity/temperature gradients changing with the tidal phase (Figure 6a and b). The tidal pumping drives vertical mixing between high nutrient deep water from the Juan de Fuca Strait and fresher surface water from the Strait of Georgia (Lewis, 1978; Murray et al., 2015; Mackas and Harrison, 1997). Nutrient concentrations in the surface Georgia Strait vary seasonally and are depleted during the summer at the stratified, fresher surface (Del Bel Belluz et al., 2021; Mackas and Harrison, 1997). Our temperature-salinity plot in August 2021 reflects end-member mixing between more saline/colder water from the Juan de Fuca Strait with fresher/warmer surface water from the Georgia Strait (Figure S9). The influence of Georgia Strait surface water is recognized by the salinity minima originating from the outflow of the Fraser River (Figures S10; Mackas and Harrison, 1997). The nitrate profiles in August 2021, though collected with a lower vertical resolution, do show diurnal variability in vertical gradients similar to salinity/temperature, consistent with the tidal mixing effect (Figure 6c).

The δ^{15}N of nitrate measured at stations near Friday Harbor also corroborate the mixing of nitrate-rich deeper water with nitrate-deplete surface water from Georgia Strait. The apparent isotope effect for nitrate assimilation in August 2021 was ~1.5 ‰, markedly lower than the canonical value of 5 ‰ associated with nitrate assimilation by surface ocean phytoplankton communities (DiFiore et al., 2006; Sigman et al., 1999; Altabet and François, 1994). A low apparent isotope effect is consistent with two end-member mixing of lower δ^{15}N, nitrate-rich water with highly fractionated (high δ^{15}N), low-nitrate water (Sigman et al., 1999). Highly fractionated nitrate, in turn,

likely originated from nutrient-depleted Georgia Strait surface waters entrained into the Channel Islands. The linear relationship between salinity and nitrate concentration in August 2021 further substantiates physical mixing as the dominant control on nitrate concentrations and isotope ratios in San Juan Channel (Figure S10; Mackas and Harrison, 1997). Moreover, the $\delta^{15}N$ of nitrate was relatively uniform with depth, indicating effective vertical mixing of the Georgia Strait and Juan de Fuca Strait water masses. The relatively slight decrease in nitrate $\delta^{15}N$ with depth suggests a secondary influence of local nitrate assimilation on its concentration and isotope ratios.

The corresponding $\delta^{15}N$ of SPOM at Friday Harbor covered a broad range, from 4.2 ‰ to 8.7 ‰ in August 2021. The depth distribution of SPOM did not mirror the corresponding nitrate $\delta^{15}N$ profile, as could otherwise be expected. At the stratified near-surface (5 m) at station 1, the $\delta^{15}N$ of SPOM averaged 4.2 ‰ compared to 7.4 ‰ for nitrate. In the context of Rayleigh fractionation, this result suggests that particulate material at the surface consisted primarily of the instantaneous product of nitrate assimilation (Mariotti et al., 1981). The lower $\delta^{15}N$ SPOM values could also reflect some degree of reliance on regenerated N species, which would result in $\delta^{15}N$ of SPOM lower than that of incident nitrate (Fawcett et al., 2011; Lourey et al., 2003; Treibergs et al., 2014). Deeper in the water column, the $\delta^{15}N$ of SPOM converged on the $\delta^{15}N$ of incident nitrate, between 6 and 7‰, suggesting that SPOM derived from the complete consumption of an incident nitrate pool (even though nitrate was present at these depths). Phytoplankton at these depths may thus have originated from surface water entrained from the Strait of Georgia – where nitrate was completely utilized. The above dynamics complicate validation of the offset between $\delta^{15}N$ of exported PON and coral-bound $\delta^{15}N$. Yet we find little evidence for nitrate fractionation from partial assimilation on $\delta^{15}N$ of phytoplankton SPOM, which suggests that the $\delta^{15}N$ imparted on local *B. elegans* skeletons should reflect the $\delta^{15}N$ of nitrate entrained to the surface. The ~ 7‰ difference between coral skeleton $\delta^{15}N$ (~13.5‰) and the entrained nitrate (~6.5‰) is similar to the empirical range of 7 - 9‰ reported for other CWC species, (e.g. *D. petusa,* Kiriakoulakis et al., 2005) and *D. dianthus* (Wang et al. 2014) and suggests that *B. elegans* provides a record of the thermocline nitrate $\delta^{15}N$ and surface nutrient dynamics at Friday Harbor.

5. Conclusions and implications for paleo-reconstruction from coral $\delta^{15}N$

We conclude that the solitary scleractinian cold water coral *B. elegans* in Friday Harbor, WA predominantly derives nutrition from metazoan zooplankton prey. While our study was limited to a shallow field site, our isotope feeding experiment, evaluated alongside previously published studies, points to the possibility that

deeper-dwelling CWCs could also rely on zooplankton prey as a fundamental component of their diet. SPOM may contribute to these CWCs' diet, but it cannot be presumed to exclusively account for the large offset between $\delta^{15}N$ of PON export and coral skeleton $\delta^{15}N$ documented by Wang et al. (2014). The $\delta^{15}N$ of skeletal material recovered from coral archives is thus likely to be sensitive to local food web dynamics; for a given $\delta^{15}N$ of sinking PON exiting the surface ocean, the $\delta^{15}N$ recorded by CWC may differ among individuals of the same species feeding on different zooplankton prey, depending on availability. In fact, Wang et al. (2014) did report a "natural variability" of 1-1.5‰ within a single specimen that might have resulted from some variability of the local food web on a short time scale of few years. Some studies have documented an increase in the degree of carnivory of zooplankton with depth (Dodds et al., 2009; Vinogradov, 1962). For instance, Hannides et al. (2013) recorded a 3.5 ‰ increase in zooplankton $\delta^{15}N$ from 150 m to 1000 m in the Subtropical North Pacific, with the steepest rate of increase from 100 – 300 m. Koppelmann et al. (2009) reported a similar pattern of zooplankton $\delta^{15}N$ through the water column. These findings could explain previous reports of small but resolvable (1-2 ‰) depth-dependencies of coral $\delta^{15}N$ (Wang et al. 2014) if corals feed predominantly on zooplankton with depth-dependent degree of carnivory of zooplankton and increasing with depth $\delta^{15}N$. The $\delta^{15}N$ recorded in CWC skeletons also tends to differ among species by 1-2‰, as respective species occupy different nutritional niches (Teece et al., 2011). The relationship between CWC species represented in fossil archives to the depth structure of their zooplankton prey warrants further investigation.

Consideration of the possible dependence of coral-bound $\delta^{15}N$ on food web dynamics informs the questions that can be competently addressed by this proxy. Although we do not have direct estimates of the $\delta^{15}N$ range that can be expected from local food web variability, the scatter around the global compilation of Wang et al. (2014) for coral-bound $\delta^{15}N$ of *D. dianthus* relative to the $\delta^{15}N$ of PON suggests that this range is modest, on the order of ~1-2 ‰. Given this range, we suggest that the coral-bound $\delta^{15}N$ proxy will be most useful for reconstructing larger environmental $\delta^{15}N$ signals and where chosen coral samples belong to the same species and are collected at comparable depths as has already been successfully demonstrated by Wang et al. (2017), Studer et al. (2018) and Chen et al. (2023). If used in this way, the broad geographic and temporal coverage afforded by CWCs, the opportunity to measure multiple proxies from individual specimens and the imperviousness of coral-bound $\delta^{15}N$ to diagenetic alteration render it a valuable paleo-proxy for reconstructing marine N cycling.

Data Availability Data presented in this paper is available at: https://www.bco-dmo.org/project/893811

Author Contribution JG, AG, and MP conceptualized the research presented in this paper. JM and AG designed and carried out culture experiments. MP and AC prepared coral samples for analysis. JM and VR analyzed samples. JM, AG, JG and KD collected water samples, SPOM, and net tows. KD collected live corals for culture experiments and field studies. JM and JG prepared the manuscript with contributions from all co-authors.

Competing Interests: The authors declare that they have no conflict of interest.

Acknowledgements

We are grateful to Friday Harbor Labs for their assistance with coral collections and field sampling, especially Pema Kitaeff and Megan Dethier. We acknowledge the valued assistance of the Artemia Reference Center (specifically Gilbert Van Stappen and Christ Mahieu). Coral culture experiments would not have been sustained without the help of St. Olaf undergraduate students Rachel Raser, Joash Daniel, Qintiantian Nong, YiWynn Chan, Mansha Haque, Natasia Preys and Miranda Lenz. We are also indebted to Dr. C. Tobias and P. Ruffino for access to and assistance with the Elemental Analyzer Isotope Ratio Mass Spectrometer. This projected was funded by an NSF RUI award to A.G. (OCE-1949984), M.G.P (OCE-1949132) and J.G. (OCE-1949119).

References

Adams, T.S., Sterner, R.W. 2000. The effect of dietary nitrogen content on trophic level ^{15}N enrichment. Limnol. Oceanogr. 45, 601–607. https://doi.org/10.4319/lo.2000.45.3.0601

Adkins, J.F., Henderson, G.M., Wang, S.-L., O'Shea, S., Mokadem, F. 2004. Growth rates of the deep-sea Scleractinia *Desmophyllum cristagalli* and *Enallopsammia rostrata*. Earth and Planetary Science Letters 227, 481-490. https://doi.org/10.1016/j.epsl.2004.08.022

Al-Moghrabi, S., Allemand, D. & Jaubert, J. 1993. Valine uptake by the scleractinian coral *Galaxea fascicularis:* characterization and effect of light and nutritional status. *J Comp Physiol B* **163**, 355–362. https://doi.org/10.1007/BF00265638

Altabet, M.A., 1988. Variations in nitrogen isotopic composition between sinking and suspended particles: implications for nitrogen cycling and particle transformation in the open ocean. Deep Sea Res. Part Oceanogr. Res. Pap. 35, 535–554. https://doi.org/10.1016/0198-0149(88)90130-6

Altabet, M.A., Deuser, W.G., Honjo, S., Stienen, C., 1991. Seasonal and depth-related changes in the source of sinking particles in the North Atlantic. Nature 354, 136–139. https://doi.org/10.1038/354136a0

Altabet, M.A., Francois, R., 1994. Sedimentary nitrogen isotopic ratio as a recorder for surface ocean nitrate utilization. Glob. Biogeochem. Cycles 8, 103–116. https://doi.org/10.1029/93GB03396

Altabet, M., Higginson, M. & Murray, D. 2002. The effect of millennial-scale changes in Arabian Sea denitrification on atmospheric CO_2. *Nature* **415**, 159–162. https://doi.org/10.1038/415159a

Ayliffe, L.K., Cerling, T.E., Robinson, T., West, A.G., Sponheimer, M., Passey, B.H., Hammer, J., Roeder, B., Dearing, M.D., Ehleringer, J.R., 2004. Turnover of carbon isotopes in tail hair and breath CO2 of horses fed an isotopically varied diet. Oecologia 139, 11–22. https://doi.org/10.1007/s00442-003-1479-x

745 Beauchamp, K.A., 1989. Aspects of gametogenesis, development and planulation in laboratory populations of
746   solitary corals and corallimorpharian sea anemones (Ph.D.). University of California, Santa Cruz, United
747   States - California.

748 Böhlke, J.K., Mroczkowski, S.J., Coplen, T.B., 2003. Oxygen isotopes in nitrate: new reference materials for
749   18O:17O:16O measurements and observations on nitrate-water equilibration. Rapid Commun. Mass
750   Spectrom. RCM 17, 1835–1846. https://doi.org/10.1002/rcm.1123

751 Braman, R.S., Hendrix, S.A., 1989. Nanogram nitrite and nitrate determination in environmental and biological
752   materials by vanadium(III) reduction with chemiluminescence detection. Anal. Chem. 61, 2715–2718.
753   https://doi.org/10.1021/ac00199a007

754 Brandes, J.A., Devol, A.H., 2002. A global marine-fixed nitrogen isotopic budget: Implications for Holocene
755   nitrogen cycling. Glob. Biogeochem. Cycles 16, 67-1-67–14. https://doi.org/10.1029/2001GB001856

756 Bronk, D. A. 2002. Dynamics of DON. Biogeochem. Mar. Dissolved Org. Matter 153–249.

757 Brown, B. E., & Bythell, J. C. 2005. Perspectives on mucus secretion in reef corals. *Marine Ecology Progress
758   Series*, *296*, 291–309. doi:10.3354/meps296291

759 Cairns, S.D., 2007. Deep-water corals: an overview with special reference to diversity and distribution of deep-
760   water scleractinian corals. Bull. Mar. Sci. 81, 311–322.

761 Carlier, A., Guilloux, E.L., Olu, K., Sarrazin, J., Mastrototaro, F., Taviani, M., Clavier, J., 2009. Trophic
762   relationships in a deep Mediterranean cold-water coral bank (Santa Maria di Leuca, Ionian Sea). Mar.
763   Ecol. Prog. Ser. 397, 125–137. https://doi.org/10.3354/meps08361

764 Carpenter, E. J., Harvey, H. R., Fry, B. & Capone, D. G. 1997. Biogeochemical tracers of the marine
765   cyanobacterium Trichodesmium. Deep-Sea Res. I 44, 27–38. doi.org/10.1016/S0967-0637(96)00091-X

766 Casciotti, K.L., Sigman, D.M., Hastings, M.G., Böhlke, J.K., Hilkert, A., 2002. Measurement of the oxygen
767   isotopic composition of nitrate in seawater and freshwater using the denitrifier method. Anal. Chem. 74,
768   4905–4912. https://doi.org/10.1021/ac020113w

769 Casciotti, K.L., Trull, T.W., Glover, D.M., Davies, D., 2008. Constraints on nitrogen cycling at the subtropical
770   North Pacific Station ALOHA from isotopic measurements of nitrate and particulate nitrogen. Deep Sea
771   Res. Part II Top. Stud. Oceanogr. 55, 1661–1672. https://doi.org/10.1016/j.dsr2.2008.04.017

772 Cathalot C, Van Oevelen D, Cox TJS, Kutti T., Lavaleye M., Duineveld G., Meysman F. J. R. 2015. Cold-water
773   coral reefs and adjacent sponge grounds: hotspots of benthic respiration and organic carbon cycling in the
774   deep sea. *Front Mar Sci* 2. https://www.frontiersin.org/articles/10.3389/fmars.2015.00037.

775 Cerling, T.E., Ayliffe, L.K., Dearing, M.D., Ehleringer, J.R., Passey, B.H., Podlesak, D.W., Torregrossa, A-M.,
776   West, A.G. 2007. Determining biological tissue turnover using stable isotopes: the reaction progress
777   variable. Ecophysiology 151, 175-189. https://doi.org/10.1007/s00442-006-0571-4

778 Chen, WH., Ren, H., Chiang, J.C.H. *et al.* Increased tropical South Pacific western boundary current transport
779   over the past century. *Nat. Geosci.* **16**, 590–596 (2023). https://doi.org/10.1038/s41561-023-01212-4

780 Cheng, H., Adkins, J., Edwards, R.L., Boyle, E.A., 2000. U-Th dating of deep-sea corals. Geochim. Cosmochim.
781   Acta 64, 2401–2416. https://doi.org/10.1016/S0016-7037(99)00422-6

Crook, E.D., Cooper, H., Potts, D.C., Lambert, T., Paytan, A., 2013. Impacts of food availability and pCO2 on planulation, juvenile survival, and calcification of the azooxanthellate scleractinian coral Balanophyllia elegans. Biogeosciences 10, 7599–7608. https://doi.org/10.5194/bg-10-7599-2013

Da Ros, Z., Dell'Anno, A., Fanelli, E., Angeletti, L., Taviani, M., Danovaro, R., 2022. Food preferences of Mediterranean cold-water corals in captivity. Front. Mar. Sci. 9. https://doi.org/10.3389/fmars.2022.867656

Del Bel Belluz, J., Peña, M.A., Jackson, J.M., Nemcek, N., 2021. Phytoplankton composition and environmental drivers in the Northern Strait of Georgia (Salish Sea), British Columbia, Canada. Estuaries Coasts 44, 1419–1439. https://doi.org/10.1007/s12237-020-00858-2

De Pol-Holz R, Robinson RS, Hebbeln D, Sigman DM, Ulloa O. 2009. Controls on sedimentary nitrogen isotopes along the Chile margin. *Deep Res Part II Top Stud Oceanogr* 56(16). doi:10.1016/j.dsr2.2008.09.014

DiFiore, P.J., Sigman, D.M., Trull, T.W., Lourey, M.J., Karsh, K., Cane, G., Ho, R., 2006. Nitrogen isotope constraints on subantarctic biogeochemistry. J. Geophys. Res. Oceans 111. https://doi.org/10.1029/2005JC003216

Dodds, L.A., Black, K.D., Orr, H., Roberts, J.M., 2009. Lipid biomarkers reveal geographical differences in food supply to the cold-water coral *Lophelia pertusa* (Scleractinia). Mar. Ecol. Prog. Ser. 397, 113–124. https://doi.org/10.3354/meps08143

Doi, H., Akamatsu, F., González, A.L., 2017. Starvation effects on nitrogen and carbon stable isotopes of animals: an insight from meta-analysis of fasting experiments. R. Soc. Open Sci. 4, 170633. https://doi.org/10.1098/rsos.170633

Drake, J.L., Guillermic, M., Eagle, R.A., Jacobs, D.K., 2021. Fossil corals with various degrees of preservation can retain information about biomineralization-related organic material. Front. Earth Sci. 9. https://doi.org/10.3389/feart.2021.643864

Druffel, E.R.M., 1997. Geochemistry of corals: Proxies of past ocean chemistry, ocean circulation, and climate. Proc. Natl. Acad. Sci. 94, 8354–8361. https://doi.org/10.1073/pnas.94.16.8354

Duineveld, G.C.A., Lavaleye, M.S.S., Berghuis, E.M., 2004. Particle flux and food supply to a seamount cold-water coral community (Galicia Bank, NW Spain). Mar. Ecol. Prog. Ser. 277, 13–23. https://doi.org/10.3354/meps277013

Duineveld, G., Lavaleye, M., Bergman, M., Stigter, H., Mienis, F., 2007. Trophic structure of a cold-water coral mound community (Rockall Bank, NE Atlantic) in relation to the near-bottom particle supply and current regime. Bull. Mar. Sci. 81, 449–467.

Durham, J. W., and Barnard, J.L., 1952. Stony corals of the Eastern Pacific collected by the Velero III and Velero IV. Al1an Hancock Pacific Expeditions 16, 1-110.

Erler, D.V., Wang, X.T., Sigman, D.M., Scheffers, S.R., Shepherd, B.O., 2015. Controls on the nitrogen isotopic composition of shallow water corals across a tropical reef flat transect. Coral Reefs 34, 329–338. https://doi.org/10.1007/s00338-014-1215-5

819   Esri. "Ocean" [basemap]. Scale Not Given. " Ocean Basemap ". February 11, 2021.
820   https://hub.arcgis.com/maps/CESPK::ocean-basemap/explore?location=35.956244%2C-
821   111.078800%2C5.00. (December, 2022).

822   Fadlallah, Y.H., 1983. Population Dynamics and Life History of a Solitary Coral, *Balanophyllia elegans*, from
823   Central California. Oecologia 58, 200–207. https://doi.org/10.1007/BF00399217

824   Fautin, D.G., 2009. Structural diversity, systematics, and evolution of cnidae. Toxicon, Cnidarian Toxins and
825   Venoms 54, 1054–1064. https://doi.org/10.1016/j.toxicon.2009.02.024

826   Fawcett, S.E., Lomas, M.W., Casey, J.R., Ward, B.B., Sigman, D.M., 2011. Assimilation of upwelled nitrate by
827   small eukaryotes in the Sargasso Sea. Nat. Geosci. 4, 717–722. https://doi.org/10.1038/ngeo1265

828   Ferrier, M.D. 1991. Net uptake of dissolved free amino acids by four scleractinian corals. *Coral Reefs* **10**, 183–
829   187. https://doi.org/10.1007/BF00336772

830   François, R., Altabet, M.A., Yu, E.-F., Sigman, D.M., Bacon, M.P., Frank, M., Bohrmann, G., Bareille, G.,
831   Labeyrie, L.D., 1997. Contribution of Southern Ocean surface-water stratification to low atmospheric
832   CO2 concentrations during the last glacial period. Nature 389, 929–935. https://doi.org/10.1038/40073

833   Freiwald, A. 2002. Reef-Forming Cold-Water Corals. In: Wefer, G., Billett, D., Hebbeln, D., Jørgensen, B.B.,
834   Schlüter, M., van Weering, T.C.E. (eds) Ocean Margin Systems. Springer, Berlin, Heidelberg.
835   https://doi.org/10.1007/978-3-662-05127-6_23

836   Gagnon, A.C., Gothmann, A.M., Branson, O., Rae, J.W.B., Stewart, J.A., 2021. Controls on boron isotopes in a
837   cold-water coral and the cost of resilience to ocean acidification. Earth and Planetary Science Letters
838   554, 116662. https://doi.org/10.1016/j.epsl.2020.116662

839   Ganeshram, R. S., and Pedersen, T. F. 1998, Glacial-interglacial variability in upwelling and bioproductivity off
840   NW Mexico: Implications for Quaternary paleoclimate, *Paleoceanography*, 13(6), 634– 645,
841   doi:10.1029/98PA02508.

842   Garcia-Herrera, N., Cornils, A., Laudien, J., Niehoff, B., Höfer, J., Försterra, G., González, H.E., Richter, C.,
843   2022. Seasonal and diel variations in the vertical distribution, composition, abundance and biomass of
844   zooplankton in a deep Chilean Patagonian Fjord. PeerJ 10, e12823. https://doi.org/10.7717/peerj.12823

845   Genin, A., Dayton, P.K., Lonsdale, P.F., Spiess, F.N., 1986. Corals on seamount peaks provide evidence of
846   current acceleration over deep-sea topography. Nature 322, 59–61. https://doi.org/10.1038/322059a0

847   Gerrodette, T. 1981. Equatorial Submergence in a Solitary Coral, Balanophyllia elegans, and the Critical Life
848   Stage Excluding the Species from Shallow Water in the South. Mar. Ecol. Prog. Series 1, 227-235.
849   http://www.jstor.org/stable/24812947.

850   Gonfiantini, R., W. Stichler, and K. Rosanski 1995, Standards and Intercomparison. Materials Distributed by the
851   IAEA for Stable Isotope Measurements,Int. At. Energy Agency, Vienna.

852   Goodfriend, G.A., Hare, P.E., Druffel, E.R.M. 1992. Aspartic acid racemization and protein diagenesis in corals
853   over the last 350 years. Geochim. Cosmochim. Acta 56, 3847–3850. https://doi.org/10.1016/0016-
854   7037(92)90176-J
855

856 Gori, A., R. Grover, C. Orejas, S. Sikorski, and C. Ferrier-Pagès. 2014. Uptake of dissolved free amino acids by
857   four cold-water coral species from the Mediterranean Sea. Deep Sea Res. Part II Top. Stud. Oceanogr.
858   **99**: 42–50. doi:10.1016/j.dsr2.2013.06.007

859 Gothmann AM, Stolarski J, Adkins JF, et al. Fossil corals as an archive of secular variations in seawater
860   chemistry since the Mesozoic. *Geochim Cosmochim Acta*. 2015;160:188-208.
861   doi:https://doi.org/10.1016/j.gca.2015.03.018

862 Grover, R. Maguer, J-F, Allemand, D., Ferrier-Pagès, C. 2008. Uptake of dissolved free amino acids by the
863   scleractinian coral *Stylophora pistillata*. *J Exp Biol* 211 (6): 860–865. doi:
864   https://doi.org/10.1242/jeb.012807

865 Hannides, Cecelia C. S., Popp, Brian N., Choy, C. Anela, Drazen, Jeffrey C. 2013. Midwater zooplankton and
866   suspended particle dynamics in the North Pacific Subtropical Gyre: A stable isotope perspective,
867   *Limnology and Oceanography*, 58, doi: 10.4319/lo.2013.58.6.1931.

868 Hill, T.M., Myrvold, C.R., Spero, H.J., Guilderson, T.P. 2014. Evidence for benthic and pelagic food web
869   coupling and carbon export from California margin bamboo coral archives. *Biogeosciences* 11, 3845–
870   3854. https://doi.org/10.5194/bg-11-3845-2014

871 Hines, S.K.V., Southon, J.R., Adkins, J.F. 2015. A high-resolution record of Southern Ocean intermediate water
872   radiocarbon over the past 30,000 years. *Earth and Planetary Science Letters* 432, 46-58.
873   https://doi.org/10.1016/j.epsl.2015.09.038

874 Hoegh-Guldberg, O., Williamson, J. Availability of two forms of dissolved nitrogen to the coral Pocillopora
875   damicornis and its symbiotic zooxanthellae. *Marine Biology* **133**, 561–570 (1999).
876   https://doi.org/10.1007/s002270050496

877 Höfer, J., González, H.E., Laudien, J., Schmidt, G.M., Häussermann, V., Richter, C., 2018. All you can eat: the
878   functional response of the cold-water coral *Desmophyllum dianthus* feeding on krill and copepods. PeerJ
879   6, e5872. https://doi.org/10.7717/peerj.5872

880 Horn, M.G., Robinson, R.S., Rynearson, T.A., Sigman, D.M., 2011. Nitrogen isotopic relationship between
881   diatom-bound and bulk organic matter of cultured polar diatoms. Paleoceanography 26.
882   https://doi.org/10.1029/2010PA002080

883 Kast, E.R., Stolper, D.A., Auderset, A., Higgins, J.A., Ren, H., Wang, X.T., Martínez-García, A., Haug, G.H.,
884   Sigman, D.M., 2019. Nitrogen isotope evidence for expanded ocean suboxia in the early Cenozoic.
885   Science 364, 386–389. https://doi.org/10.1126/science.aau5784

886 Kiriakoulakis, K., Fisher, E., Wolff, G.A., Freiwald, A., Grehan, A., Roberts, J.M., 2005. Lipids and nitrogen
887   isotopes of two deep-water corals from the North-East Atlantic: initial results and implications for their
888   nutrition, in: Freiwald, A., Roberts, J.M. (Eds.), Cold-Water Corals and Ecosystems, Erlangen Earth
889   Conference Series. Springer, Berlin, Heidelberg, pp. 715–729. https://doi.org/10.1007/3-540-27673-4_37

890 Knapp, A. N., K. L. Casciotti, and M. G. Prokopenko. 2018. Dissolved Organic Nitrogen Production and
891   Consumption in Eastern Tropical South Pacific Surface Waters. Glob. Biogeochem. Cycles **32**: 769–783.
892   doi:10.1029/2017GB005875

893 Knapp AN, DiFiore PJ, Deutsch C, Sigman DM, Lipschultz F. 2008. Nitrate isotopic composition between
894   Bermuda and Puerto Rico: Implications for N2 fixation in the Atlantic Ocean. *Global Biogeochem Cycles*
895   22(3). doi:10.1029/2007GB003107

896 Koppelmann, R., Böttger-Schnack, R., Möbius, J., Weikert, H., 2009. Trophic relationships of zooplankton in the
897   eastern Mediterranean based on stable isotope measurements. Journal of Plankton Research 31, 669-686.
898   https://doi.org/10.1093/plankt/fbp013

899 Lasker, H.R., 1981. A comparison of the particulate feeding abilities of three species of Gorgonian soft coral.
900   Mar. Ecol. Prog. Ser. 5, 61–67. doi:10. 3354/meps005061

901 Lewis, A.G., 1978. Concentrations of nutrients and chlorophyll on a cross-channel transect in Juan de Fuca Strait,
902   British Columbia. J. Fish. Res. Board Can. 35, 305–314. https://doi.org/10.1139/f78-055

903 Lewis, J.B., Price, W.S., 1975. Feeding mechanisms and feeding strategies of Atlantic reef corals. J. Zool. 176,
904   527–544. https://doi.org/10.1111/j.1469-7998.1975.tb03219.x

905 Li, T., Robinson, L.F., Chen, T., Wang, X.T., Burke, A., Rae, J.W.B., Pegrum-Haram, A., Knowles, T.D.J., Li,
906   G., Chen, J., Ng, H.C., Prokopenko, M., Rowland, G.H., Samperiz, A., Stewart, J.A., Southon, J.,
907   Spooner, P.T., 2020. Rapid shifts in circulation and biogeochemistry of the Southern Ocean during
908   deglacial carbon cycle events. Science Advances 6, eabb3807. DOI: 10.1126/sciadv.abb3807

909 Lourey, M.J., Trull, T.W., Sigman, D.M., 2003. Sensitivity of $\delta15N$ of nitrate, surface suspended and deep
910   sinking particulate nitrogen to seasonal nitrate depletion in the Southern Ocean. Glob. Biogeochem.
911   Cycles 17. https://doi.org/10.1029/2002GB001973

912 Mackas, D.L., Harrison, P.J., 1997. Nitrogenous nutrient sources and sinks in the Juan de Fuca Strait/Strait of
913   Georgia/Puget Sound estuarine system: Assessing the potential for eutrophication. Estuar. Coast. Shelf
914   Sci. 44, 1–21. https://doi.org/10.1006/ecss.1996.0110

915 Maier, S.R., Bannister, R.J., van Oevelen, D., Kutti, T., 2020. Seasonal controls on the diet, metabolic activity,
916   tissue reserves and growth of the cold-water coral *Lophelia pertusa*. Coral Reefs 39, 173–187.
917   https://doi.org/10.1007/s00338-019-01886-6

918 Maier, S.R., Kutti, T., Bannister, R.J., van Breugel, P., van Rijswijk, P., van Oevelen, D., 2019. Survival under
919   conditions of variable food availability: Resource utilization and storage in the cold-water coral *Lophelia*
920   *pertusa*. Limnol. Oceanogr. 64, 1651–1671. https://doi.org/10.1002/lno.11142

921 Maier, S.R., Brooke, S., De Clippele, L.H., de Froe, E., van der Kaaden, A.-S., Kutti, T., Mienis, F., van Oevelen,
922   D., 2023. On the paradox of thriving cold-water coral reefs in the food-limited deep sea. Biological
923   Reviews 98, 1768–1795. https://doi.org/10.1111/brv.12976

924 Marconi D, Weigand AM, Rafter PA, Matthew R. McIlvin MR, Matthew Forbes, M Casciotti, KL Sigman, DM.
925   2015. Nitrate isotope distributions on the US GEOTRACES North Atlantic cross-basin section: Signals of
926   polar nitrate sources and low latitude nitrogen cycling. *Mar Chem*. 177:143-156.
927   doi:https://doi.org/10.1016/j.marchem.2015.06.007

928 Margolin, A. R., L. F. Robinson, A. Burke, R. G. Waller, K. M. Scanlon, M. L. Roberts, M. E. Auro, and T. van
929   de Flierdt. 2014. Temporal and spatial distributions of cold-water corals in the Drake Passage: Insights

from the last 35,000 years. Deep Sea Res. Part II Top. Stud. Oceanogr. **99**: 237–248.
doi:10.1016/j.dsr2.2013.06.008

Mariotti, A., Germon, J.C., Hubert, P., Kaiser, P., Letolle, R., Tardieux, A., Tardieux, P., 1981. Experimental
determination of nitrogen kinetic isotope fractionation: Some principles; illustration for the
denitrification and nitrification processes. Plant Soil 62, 413–430. https://doi.org/10.1007/BF02374138

Martínez del Rio, C., Carleton, S.A., 2012. How fast and how faithful: the dynamics of isotopic incorporation
into animal tissues. J. Mammal. 93, 353–359. https://doi.org/10.1644/11-MAMM-S-165.1

McCutchan Jr, J.H., Lewis Jr, W.M., Kendall, C., McGrath, C.C., 2003. Variation in trophic shift for stable
isotope ratios of carbon, nitrogen, and sulfur. Oikos 102, 378–390. https://doi.org/10.1034/j.1600-
0706.2003.12098.x

McIlvin, M.R., Casciotti, K.L., 2011. Technical Updates to the Bacterial Method for Nitrate Isotopic Analyses.
Anal. Chem. 83, 1850–1856. https://doi.org/10.1021/ac1028984

McMahon, K.W., Williams, B., Guilderson, T.P., Glynn, D.S., McCarthy, M.D., 2018. Calibrating amino acid
δ13C and δ15N offsets between polyp and protein skeleton to develop proteinaceous deep-sea corals as
paleoceanographic archives. Geochim. Cosmochim. Acta 220, 261–275.
https://doi.org/10.1016/j.gca.2017.09.048

Middelburg, J., Mueller, C., Veuger, B. Larsson, A. I., Form, A., van Oevelen, D 2016.. Discovery of symbiotic
nitrogen fixation and chemoautotrophy in cold-water corals. *Sci Rep* **5**, 17962 (2016).
https://doi.org/10.1038/srep17962

Miller, M., 1995. Growth of a temperate coral: effects of temperature, light, depth, and heterotrophy. Mar. Ecol.
Prog. Ser. 122, 217–225. https://doi.org/10.3354/meps122217

Minagawa, M., Wada, E., 1984. Stepwise enrichment of 15N along food chains: Further evidence and the relation
between δ15N and animal age. Geochim. Cosmochim. Acta 48, 1135–1140.
https://doi.org/10.1016/0016-7037(84)90204-7

Mortensen P.B., (2001) Aquarium observations on the deep-water coral *Lophelia pertusa* (L., 1758) (scleractinia)
and selected associated invertebrates, Ophelia, 54:2, 83-104, DOI: 10.1080/00785236.2001.10409457

Muhs, D.R., Kennedy, G.L., Rockwell, T.K., 1994. Uranium-Series Ages of Marine Terrace Corals from the
Pacific Coast of North America and Implications for Last-Interglacial Sea Level History. Quaternary
Research 42, 72–87. https://doi.org/10.1006/qres.1994.1055

Mueller, C.E., Larsson, A.I., Veuger, B., Middelburg, J.J., van Oevelen, D., 2014. Opportunistic feeding on
various organic food sources by the cold-water coral *Lophelia pertusa*. Biogeosciences 11, 123–133.
https://doi.org/10.5194/bg-11-123-2014

Murray, J.W., Roberts, E., Howard, E., O'Donnell, M., Bantam, C., Carrington, E., Foy, M., Paul, B., Fay, A.,
2015. An inland sea high nitrate-low chlorophyll (HNLC) region with naturally high pCO2. Limnol.
Oceanogr. 60, 957–966. https://doi.org/10.1002/lno.10062

Muscatine, L., Goiran, C., Land, L., Jaubert, J., Cuif, J.-P., Allemand, D., 2005. Stable isotopes (δ13C and δ15N)
of organic matrix from coral skeleton. Proc. Natl. Acad. Sci. 102, 1525–1530.
https://doi.org/10.1073/pnas.0408921102

968 Naumann, M.S., Orejas, C., Wild, C., Ferrier-Pagès, C., 2011. First evidence for zooplankton feeding sustaining
969 key physiological processes in a scleractinian cold-water coral. J. Exp. Biol. 214, 3570–3576.
970 https://doi.org/10.1242/jeb.061390

971 Naumann, M.S., Tolosa, I., Taviani, M., Grover, R., Ferrier-Pagès, C., 2015. Trophic ecology of two cold-water
972 coral species from the Mediterranean Sea revealed by lipid biomarkers and compound-specific isotope
973 analyses. Coral Reefs 34, 1165–1175. https://doi.org/10.1007/s00338-015-1325-8

974 Pride C, Thunell R, Sigman D, Keigwin L, Altabet M, Tappa E. 1999. Nitrogen isotopic variations in the Gulf of
975 California since the Last Deglaciation: Response to global climate change. *Paleoceanography* 14(3).
976 doi:10.1029/1999PA900004

977 Purser A, Larsson AI, Thomsen L, van Oevelen D. 2010. The influence of flow velocity and food concentration
978 on *Lophelia pertusa* (Scleractinia) zooplankton capture rates. *J Exp Mar Bio Ecol*. 395(1):55-62.
979 doi:https://doi.org/10.1016/j.jembe.2010.08.013

980 Rae, J.W.B. 2018. Boron Isotopes in Foraminifera: Systematics, Biomineralisation, and CO_2 Reconstruction. In:
981 Marschall, H., Foster, G. (eds) Boron Isotopes. Advances in Isotope Geochemistry. Springer, Cham.
982 https://doi.org/10.1007/978-3-319-64666-4_5

983 Rangel, M.S., Erler, D., Tagliafico, A., Cowden, K., Scheffers, S., Christidis, L., 2019. Quantifying the transfer
984 of prey δ15N signatures into coral holobiont nitrogen pools. Mar. Ecol. Prog. Ser. 610, 33–49.
985 https://doi.org/10.3354/meps12847

986 Ren, H., Sigman, D.M., Meckler, A.N., Plessen, B., Robinson, R.S., Rosenthal, Y., Haug, G.H., 2009.
987 Foraminiferal Isotope Evidence of Reduced Nitrogen Fixation in the Ice Age Atlantic Ocean. Science
988 323, 244–248. https://doi.org/10.1126/science.1165787

989 Reynaud, S., Martinez, P., Houlbrèque, F., Billy, I., Allemand, D., Ferrier-Pagès, C., 2009. Effect of light and
990 feeding on the nitrogen isotopic composition of a zooxanthellate coral: role of nitrogen recycling. Mar.
991 Ecol. Prog. Ser. 392, 103–110. https://doi.org/10.3354/meps08195

992 Roberts, J.M., Wheeler, A.J., Freiwald, A., 2006. Reefs of the deep: The biology and geology of cold-water coral
993 ecosystems. Science 312, 543–547. https://doi.org/10.1126/science.1119861

994 Robinson, R.S., Kienast, M., Albuquerque, A.L., Altabet, M., Contreras, S., Holz, R.D.P., Dubois, N., Francois,
995 R., Galbraith, E., Hsu, T.-C., Ivanochko, T., Jaccard, S., Kao, S.-J., Kiefer, T., Kienast, S., Lehmann, M.,
996 Martinez, P., McCarthy, M., Möbius, J., Pedersen, T., Quan, T.M., Ryabenko, E., Schmittner, A.,
997 Schneider, R., Schneider-Mor, A., Shigemitsu, M., Sinclair, D., Somes, C., Studer, A., Thunell, R., Yang,
998 J.-Y., 2012. A review of nitrogen isotopic alteration in marine sediments. Paleoceanography 27.
999 https://doi.org/10.1029/2012PA002321

1000 Robinson LF, Adkins JF, Frank N, Gagnon, A.C., Prouty, N.G., Roark, B. van de Flierdt, T. 2014. The
1001 geochemistry of deep-sea coral skeletons: A review of vital effects and applications for
1002 palaeoceanography. *Deep Sea Res Part II Top Stud Oceanogr*. 99:184-198.
1003 doi:https://doi.org/10.1016/j.dsr2.2013.06.005

1004 Robinson RS, Sigman DM. 2008. Nitrogen isotopic evidence for a poleward decrease in surface nitrate within the
1005 ice age Antarctic. *Quat Sci Rev*. 27(9-10). doi:10.1016/j.quascirev.2008.02.005

1006 Robinson, R.S., Smart, S.M., Cybulski, J.D., McMahon, K.W., Marcks, B., Nowakowski, C., 2023. Insights from
1007   fossil-bound nitrogen isotopes in diatoms, foraminifera, and corals. Annu. Rev. Mar. Sci. 15, null.
1008   https://doi.org/10.1146/annurev-marine-032122-104001

1009 Ryan, W. B. F., S.M. Carbotte, J. Coplan, S. O'Hara, A. Melkonian, R. Arko, R.A. Weissel, V. Ferrini, A.
1010   Goodwillie, F. Nitsche, J. Bonczkowski, R. Zemsky, 2009. Global Multi-Resolution Topography
1011   (GMRT) synthesis data set, *Geochem. Geophys. Geosyst.*, 10, Q03014, doi:10.1029/2008GC002332.

1012 Saino, T., Hattori, A., 1987. Geographical variation of the water column distribution of suspended particulate
1013   organic nitrogen and its 15N natural abundance in the Pacific and its marginal seas. Deep Sea Res. A 34,
1014   807–827. https://doi.org/10.1016/0198-0149(87)90038-0

1015 Scrimgeour, C.M., Gordon, S.C., Handley, L.L., Woodford, J.A.T., 1995. Trophic levels and anomalous δ15N of
1016   insects on raspberry (Rubus Idaeus L.). Isotopes Environ. Health Stud. 31, 107–115.
1017   https://doi.org/10.1080/10256019508036256

1018 Sebens, K.P., Vandersall, K.S., Savina, L.A., Graham, K.R., 1996. Zooplankton capture by two scleractinian
1019   corals, Madracis mirabilis andMontastrea cavernosa, in a field enclosure. Mar. Biol. 127, 303–317.
1020   https://doi.org/10.1007/BF00942116

1021 Sherwood, O.A., Heikoop, J.M., Scott, D.B., Risk, M.J., Guilderson, T.P., McKinney, R.A., 2005. Stable isotopic
1022   composition of deep-sea gorgonian corals *Primnoa* spp.: a new archive of surface processes. Mar. Ecol.
1023   Prog. Ser. 301, 135–148. https://doi.org/10.3354/meps301135

1024 Sherwood, O.A., Jamieson, R.E., Edinger, E.N., Wareham, V.E., 2008. Stable C and N isotopic composition of
1025   cold-water corals from the Newfoundland and Labrador continental slope: Examination of trophic, depth
1026   and spatial effects. Deep Sea Res. Part Oceanogr. Res. Pap. 55, 1392–1402.
1027   https://doi.org/10.1016/j.dsr.2008.05.013

1028 Sherwood, O.A., Thresher, R.E., Fallon, S.J., Davies, D.M., Trull, T.W., 2009. Multi-century time-series of ^{15}N
1029   and ^{14}C in bamboo corals from deep Tasmanian seamounts: evidence for stable oceanographic
1030   conditions. Mar. Ecol. Prog. Ser. 397, 209–218. https://doi.org/10.3354/meps08166

1031 Sigman, D.M., Altabet, M.A., McCorkle, D.C., Francois, R., Fischer, G., 1999. The δ^{15}N of nitrate in the
1032   Southern Ocean: Consumption of nitrate in surface waters. Glob. Biogeochem. Cycles 13, 1149–1166.
1033   https://doi.org/10.1029/1999GB900038

1034 Sigman, D., Boyle, E. Glacial/interglacial variations in atmospheric carbon dioxide. 2000. *Nature* **407**, 859–869
1035   (2000). https://doi.org/10.1038/35038000

1036 Sigman, D.M., Casciotti, K.L., Andreani, M., Barford, C., Galanter, M., Böhlke, J.K., 2001. A Bacterial method
1037   for the nitrogen isotopic analysis of nitrate in seawater and freshwater. Anal. Chem. 73, 4145–4153.
1038   https://doi.org/10.1021/ac010088e

1039 Sigman, D.M., Fripiat, F., 2019. *Nitrogen Isotopes in the Ocean*, in: Cochran, J.K., Bokuniewicz, H.J., Yager,
1040   P.L. (Eds.), Encyclopedia of Ocean Sciences (Third Edition). Academic Press, Oxford, pp. 263–278.
1041   https://doi.org/10.1016/B978-0-12-409548-9.11605-7

1042 Soetaert, K., Mohn, C., Rengstorf, A., Grehan, A., van Oevelen, D., 2016. Ecosystem engineering creates a direct
1043   nutritional link between 600-m deep cold-water coral mounds and surface productivity. Sci. Rep. 6,
1044   35057. https://doi.org/10.1038/srep35057

1045 Spero, H.J., Andreasen, D.J., Sorgeloos, P., 1993. Carbon and nitrogen isotopic composition of different strains
1046   of *Artemia* sp. Int. J. Salt Lake Res. 2, 133. https://doi.org/10.1007/BF02905905

1047 Studer, A.S., Sigman, D.M., Martinez-Garcia, A., Thole, L.M., Michel, E., Jaccard, S.L., Lippolds, J.A., Mazaud,
1048   A., Wang, X.C.T., Robinson, L.F., Adkins, J.F., Haug, G.H., 2018. Increased nutrient supply to the
1049   Southern Ocean during the Holocene and its implications for the pre-industrial atmospheric CO2 rise.
1050   Nat Geosci 11, 756-761. https://doi.org/10.1038/s41561-018-0191-8

1051 Tanaka, Y., Miyajima, T., Koike, I., Hayashibara, T., Ogawa, H., 2006. Translocation and conservation of
1052   organic nitrogen within the coral-zooxanthella symbiotic system of Acropora pulchra, as demonstrated
1053   by dual isotope-labeling techniques. J. Exp. Mar. Biol. Ecol. 336, 110–119.
1054   https://doi.org/10.1016/j.jembe.2006.04.011

1055 Tanaka, Y., Suzuki, A., Sakai, K., 2018. The stoichiometry of coral-dinoflagellate symbiosis: carbon and nitrogen
1056   cycles are balanced in the recycling and double translocation system. ISME J. 12, 860–868.
1057   https://doi.org/10.1038/s41396-017-0019-3

1058 Teece, M.A., Estes, B., Gelsleichter, E., Lirman, D., 2011. Heterotrophic and autotrophic assimilation of fatty
1059   acids by two scleractinian corals, Montastraea faveolata and Porites astreoides. Limnol. Oceanogr. 56,
1060   1285–1296. https://doi.org/10.4319/lo.2011.56.4.1285

1061 Thiagarajan N., Subhas A. V., Southon J. R., Eiler J. M. andAdkins J. F. 2014. Abrupt pre-Bolling-Allerod
1062   warming and circulation changes in the deep ocean. Nature 511, 75–78.
1063   https://doi.org/10.1038/nature13472

1064 Thiem, Ø., Ravagnan, E., Fosså, J.H., Berntsen, J., 2006. Food supply mechanisms for cold-water corals along a
1065   continental shelf edge. J. Mar. Syst. 60, 207–219. https://doi.org/10.1016/j.jmarsys.2005.12.004

1066 Thomas, S.M., Crowther, T.W., 2015. Predicting rates of isotopic turnover across the animal kingdom: a
1067   synthesis of existing data. J. Anim. Ecol. 84, 861–870. https://doi.org/10.1111/1365-2656.12326

1068 Treibergs, L.A., Fawcett, S.E., Lomas, M.W., Sigman, D.M., 2014. Nitrogen isotopic response of prokaryotic and
1069   eukaryotic phytoplankton to nitrate availability in Sargasso Sea surface waters. Limnol. Oceanogr. 59,
1070   972–985. https://doi.org/10.4319/lo.2014.59.3.0972

1071 Tsounis G, Orejas C, Reynaud S, JM G, Allemand D, Ferrier-Pagès C. 2010. Prey-capture rates in four
1072   Mediterranean cold water corals . *Mar Ecol Prog Ser*. 398:149-155. https://doi.org/10.3354/meps08312

1073 van Oevelen, P., Duineveld, G., Lavaleye, M., Mienis, Furu, Soetaert, Karline, H., Carlo H. R., 2009. The cold-
1074   water coral community as hotspot of carbon cycling on continental margins: A food-web analysis from
1075   Rockall Bank (northeast Atlantic), *Limnology and Oceanography*, 54, doi: 10.4319/lo.2009.54.6.1829.

1076 Vinogradov, M. E. Feeding of the deep-sea zooplankton. 1962. *Rapp. Pv. Reun. Cons. Perm. Int. Exp. Mer.* **153**,
1077   114–120.

1078 Wang, X.T., Prokopenko, M.G., Sigman, D.M., Adkins, J.F., Robinson, L.F., Ren, H., Oleynik, S., Williams, B.,
1079   Haug, G.H., 2014. Isotopic composition of carbonate-bound organic nitrogen in deep-sea scleractinian
1080   corals: A new window into past biogeochemical change. Earth Planet. Sci. Lett. 400, 243–250.
1081   https://doi.org/10.1016/j.epsl.2014.05.048

Wang, X.T., Sigman, D.M., Prokopenko, M.G., Adkins, J.F., Robinson, L.F., Hines, S.K., Chai, J., Studer, A.S., Martínez-García, A., Chen, T., Haug, G.H., 2017. Deep-sea coral evidence for lower Southern Ocean surface nitrate concentrations during the last ice age. Proc. Natl. Acad. Sci. 114, 3352–3357. https://doi.org/10.1073/pnas.1615718114

Webb, S., Hedges, R., Simpson, S., 1998. Diet quality influences the $\delta^{13}C$ and $\delta^{15}N$ of locusts and their biochemical components. J. Exp. Biol. 201, 2903–2911. https://doi.org/10.1242/jeb.201.20.2903

Weigand, M.A., Foriel, J., Barnett, B., Oleynik, S., Sigman, D.M., 2016. Updates to instrumentation and protocols for isotopic analysis of nitrate by the denitrifier method. Rapid Commun. Mass Spectrom. 30, 1365–1383. https://doi.org/10.1002/rcm.7570

Williams, B., and Grottoli, A. G. 2010. Recent shoaling of the nutricline and thermocline in the western tropical Pacific, *Geophys. Res. Lett.*, 37, L22601, doi:10.1029/2010GL044867.

Zhang, R., X. T. Wang, H. Ren, J. Huang, M. Chen, and D. M. Sigman. 2020. Dissolved Organic Nitrogen Cycling in the South China Sea From an Isotopic Perspective. Glob. Biogeochem. Cycles **34**: e2020GB006551. doi:10.1029/2020GB006551

Zhou, M., Granger, J., Chang, B.X., 2022. Influence of sample volume on nitrate N and O isotope ratio analyses with the denitrifier method. Rapid Commun. Mass Spectrom. 36, e9224. https://doi.org/10.1002/rcm.9224